

# Characterization of dsRNA-induced pancreatitis model reveals the regulatory role of IRF-2 in trypsinogen5 gene transcription

Hideki Hayashi<sup>1</sup>, Tomoko Kohno<sup>1</sup>, Kiyoshi Yasui<sup>1</sup>, Hiroyuki Murota<sup>4</sup>, Tohru Kimura<sup>5</sup>, Gordon S. Duncan<sup>8</sup>, Tomoki Nakashima<sup>7</sup>, Kazuo Yamamoto<sup>8</sup>, Ichiro Katayama<sup>4</sup>, Yuhua Ma<sup>1</sup>, Koon Jiew Chua<sup>1</sup>, Takashi Suematsu<sup>1</sup>, Isao Shimokawa<sup>2</sup>, Shizuo Akira<sup>6</sup>, Yoshinao Kubo<sup>1</sup>, Tak W. Mak<sup>8,9</sup> and Toshifumi Matsuyama<sup>1,3,\*</sup>

<sup>1</sup>Division of Cytokine Signaling, Department of Molecular Biology and Immunology, <sup>2</sup>Department of Investigative Pathology, Nagasaki University Graduate School of Biomedical Science, and <sup>3</sup>the Global Center of Excellence Program at Nagasaki University

<sup>4</sup>Department of Dermatology, and <sup>5</sup>Department of Pathology, Graduate school of Medicine, and

<sup>6</sup>Department of Host Defense, Research Institute for Microbial Diseases, Osaka University, Japan.

<sup>7</sup>Department of Cell Signaling, Tokyo Medical and Dental University, Japan.

<sup>8</sup>Campbell Family Cancer Research Institute, Princess Margaret Hospital, Toronto, ON, Canada

M5G 2M9

<sup>9</sup>Co-communicating author

\*Correspondence: Toshifumi Matsuyama, M.D., Ph.D.

Division of Cytokine Signaling, Department of Molecular Microbiology and Immunology, Nagasaki University Graduate School of Biomedical Sciences, 1-12-4 Sakamoto, Nagasaki 852-8523, Japan

Telephone: +81-95-819-7079

Fax: +81-95-819-7083

E-mail: [tosim@nagasaki-u.ac.jp](mailto:tosim@nagasaki-u.ac.jp)

Characters including spaces: 38,984

## Abstract

Mice deficient for interferon regulatory factor (IRF)-2 (IRF2<sup>-/-</sup> mice) exhibit immunological abnormalities and cannot survive lymphocytic choriomeningitis virus (LCMV) infection. The pancreas of these animals is highly inflamed, a phenotype replicated by treatment with poly(I:C), a synthetic double-stranded RNA. Trypsinogen5 mRNA was constitutively up-regulated about 1,000-fold in IRF2<sup>-/-</sup> mice compared to controls, as assessed by qRT-PCR. Further knockout of the IFN $\alpha$  receptor 1 (IFNAR1) abolished the poly(I:C)-induced pancreatitis, but had no effects on the constitutive up-regulation of trypsinogen5 gene, indicating crucial type I IFN (I-IFN) signaling to elicit the inflammation. Analysis of IFNAR1<sup>-/-</sup> mice confirmed I-IFN-dependent transcriptional activation of dsRNA-sensing pattern recognition receptor genes, *MDA5*, *RIG-I*, and *TLR3*, which induced poly(I:C) dependent cell death in the acinar cells, in the absence of IRF2. We speculate that Trypsin5, the trypsinogen5 gene product, leaking from the dead acinar cells, triggers a chain reaction leading to lethal pancreatitis in the IRF2<sup>-/-</sup> mice, because it is resistant to a major endogenous trypsin inhibitor, Spink3.

## Introduction

Interferons (IFNs) are cytokines whose actions contribute to the first line of defense against infection. IFNs both render cells resistant to viral attack and regulate cell growth and differentiation (1). IFNs elicit their pleiotropic effects by regulating the expression of many interferon-stimulated genes (ISGs). IFNs themselves are controlled by interferon regulatory factors (IRFs) that also regulate the expression of ISGs. By binding to interferon-stimulated response elements (ISREs) in gene promoters, the nine known IRF family members (IRF1-9) govern the production of cytokines related to inflammation and immune responses.

When pattern recognition receptors (PRRs) such as Toll-like receptors (TLRs) and retinoic acid-inducible gene-I (RIG)-like receptors (RLR) detect pathogen ligands, these receptors are activated (2) and transduce downstream signaling activating IFNs and IRFs. Analyses using knockout (KO) mice deficient for various IRFs have revealed their physiological roles. For example, IRF2 functions mainly as a transcriptional repressor by competing for binding to ISREs with other IRFs, especially IRF9 and IRF1 (1).

IRF2-deficient (IRF2<sup>-/-</sup>) mice spontaneously develop inflammatory skin disease as they age, and die within weeks with lymphocytic choriomeningitis virus (LCMV) infection (3). Ablation of IFN $\alpha$  receptor1 (IFNAR1) or IRF9 ameliorates the skin inflammation of IRF2<sup>-/-</sup> mice, suggesting that IRF2 negatively regulates gene expression by antagonizing IRF9, which is activated by type I IFN (I-IFN) (4). However, the precise mechanisms underlying the phenotypes of IRF2<sup>-/-</sup> are not known. In this study, we found that poly(I:C)(pIC) mimicked the LCMV-induced pancreatitis, and

we have used double KO mice to explore the cause of death in pIC-treated IRF2<sup>-/-</sup> mice. Our results show that significant trypsinogen5 up-regulation in IRF2<sup>-/-</sup> mice together with I-IFN-dependent transcriptional activation of dsRNA-sensing PRRs were critical for the pIC-induced death.

## Results and Discussion

### **IRF2<sup>-/-</sup> mice show IFN-dependent poly(I:C)-induced pancreatitis and IFN-independent secretory dysfunction in pancreatic acinar cells.**

LCMV-infected IRF2<sup>-/-</sup> mice die within four weeks post-infection (3), but all IRF2<sup>-/-</sup> mice challenged intraperitoneally (i.p.) with poly(I:C) (pIC-IRF2<sup>-/-</sup> mice) died within one week (Fig.1A). Severe acute pancreatitis was apparent in pIC-IRF2<sup>-/-</sup> mice, as shown by abundant TUNEL<sup>+</sup> apoptotic cells (Fig.1B). Even in the absence of pIC, however, some abnormalities were detected in IRF2<sup>-/-</sup> pancreas as indicated by hematoxylin and eosin (HE) staining (Fig.1C) and electron microscopy (Fig.1D). A mild infiltration of inflammatory cells (particularly lymphocytes) was noted around IRF2<sup>-/-</sup> ductal cells, but this pancreatitis was not typical. The pancreatic acinar cells in untreated IRF2<sup>-/-</sup> mice were filled with eosinophilic secretory granules of heterogeneous size, whereas fewer eosinophilic granules of more uniform size were observed mainly in the apical region of WT acinar cells. Interestingly, treatment of IRF2<sup>-/-</sup> mice with the stable cholecystokinin (CCK) analogue cerulein (5) did not cause acute pancreatitis, as assessed by electron microscopy and serum amylase levels (Fig.S1A,B). Because mRNA expression of CCK receptors in IRF2<sup>-/-</sup> mice was normal (Fig.S1C), these results suggest that the secretory and/or vesicle transport systems in IRF2<sup>-/-</sup> mice are dysfunctional.

The mRNAs encoding the Ca<sup>2+</sup>-binding proteins Anxa10, Ahsg, and S100-G involved in Ca<sup>2+</sup>-dependent vesicle transport, sorting and fusion processes, were significantly up-regulated in IRF2<sup>-/-</sup> pancreas (Table S1). The secretory dysfunction observed in cerulein treated IRF2<sup>-/-</sup> mice (6),

which is due to an abnormal distribution pattern of normal levels of soluble N-ethylmaleimide-sensitive factor attachment protein receptors (SNAREs) (6) may be due to the abnormal expression of these  $\text{Ca}^{2+}$ -binding proteins in the absence of IRF2 since annexin family proteins are known to bind and regulate of (SNAREs) (7).

Skin inflammation in IRF2<sup>-/-</sup> mice was rescued by abolishing IFN signaling (4). We asked if the atypical pancreatitis in IRF2<sup>-/-</sup> mice could be similarly rescued by crossing the IRF2<sup>-/-</sup> mutants to IFNAR1-, IRF1-, or TRIF-deficient mice (3, 8, 9) to generate double knock-out (DKO) mice. Abnormal acinar granule distribution was again observed in IRF2<sup>-/-</sup>IFNAR1<sup>-/-</sup>, IRF2<sup>-/-</sup>IRF1<sup>-/-</sup>, and IRF2<sup>-/-</sup>TRIF<sup>-/-</sup> mice (Fig. 1D). Thus, the abnormal acinar structure caused by *Irf2* disruption is not mediated by IFN signaling.

To assess pancreatitis in the DKO mice, we measured serum amylase levels before and after pIC challenge (Fig.1E). Serum amylase was elevated in pIC-IRF2<sup>-/-</sup> and pIC-IRF2<sup>-/-</sup>IRF1<sup>-/-</sup> mice. However, this increase did not occur at all in pIC-IRF2<sup>-/-</sup>IFNAR1<sup>-/-</sup> mice, and only to a limited extent in pIC-IRF2<sup>-/-</sup>TRIF<sup>-/-</sup> mice. These data indicate that type I IFN signaling via IFNAR1, as well as TLR signaling via the adaptor protein TRIF, are important for the development of pIC-induced pancreatitis in IRF2<sup>-/-</sup> mice. Moreover, our results show that IRF2 regulates IFN-independent pathways affecting acinar cell secretion, as well as IFN-dependent pathways inducing pIC-mediated pancreatitis.

## Up-regulated trypsinogen5 mRNA in the pancreas of IRF2<sup>-/-</sup> mice

We used an Affymetrix DNA microarray system to compare mRNA expression in the pancreas before and after pIC injection of IRF2<sup>-/-</sup> and WT mice (Fig. 2A). In IRF2<sup>-/-</sup> mice, 14 annotated genes were up-regulated and 8 genes were down-regulated more than 10-fold (Table S1) compared to WT mice. The transcriptional profiles of genes important for the etiology of pancreatitis (10, 11) are listed in Table 1. Strikingly, trypsinogen5 mRNA was up-regulated >100-fold in pIC-IRF2<sup>-/-</sup> pancreas, a noteworthy observation because trypsinogens activate many other pancreatic enzymes, and premature intracellular activation of trypsinogens in pancreatic acinar cells triggers acute pancreatitis (10, 11). There are 20 trypsinogen genes (T1-T20) in the murine T cell receptor  $\beta$  gene locus (12), 12 of which express trypsinogen proteins (Fig.S2 right) while humans have only 3 trypsinogen genes encoding three proteins: PRSS1, PRSS2, and PRSS3 (Fig.S2 left) (13). The gene expression profile of pIC-IRF2<sup>-/-</sup> pancreas is inflammation-prone: mouse trypsinogen mRNAs of T11 (Prss3), and T4 (Trypsinogen5) were up-regulated (Table 1), the mRNA encoding cysteine protease cathepsin B (Ctsb), an enzyme that can initiate pancreatitis by activating trypsinogens (14-16), was also up-regulated (Table 1). The mRNA encoding chymotrypsin C (Ctrc) was down-regulated, and the anti-pancreatitis factor, inter  $\alpha$ -trypsin inhibitor, was also down-regulated, although the mRNA encoding Kazal type3 (Spink3), a serine protease inhibitor that blocks trypsin activity (17), was slightly up-regulated

We examined the tissue specificity and dependency on IRF2 and IFNAR1 of trypsinogen5 expression by quantitative RT-PCR. In untreated WT mice, trypsinogen5 is expressed most highly in

pancreas and skin, and modestly in spleen (Fig.S3A). In untreated IRF2<sup>-/-</sup> mice, trypsinogen5 expression in the pancreas was up-regulated ~1,000-fold compared to controls, and was not affected by IFNAR1 ablation. Trypsinogen5 mRNA was up-regulated in IRF2<sup>-/-</sup> spleen to a much lower extent than in IRF2<sup>-/-</sup> pancreas, and was not detectable in liver or lung of WT or IRF2<sup>-/-</sup> mice.

We examined the effects of various IRFs on the activity of the murine trypsinogen5 promoter which contains 7 ISREs. We cloned a 1.1kb fragment of the trypsinogen5 promoter region (-1063 to +15), to create a series of promoter deletion constructs mutants, driving the firefly luciferase reporter gene (Fig.2B left). These were transfected into HEK293T cells along with plasmids overexpressing murine IRF1, IRF5, IRF7 or MyD88. MyD88 was required for IRF-mediated activation of trypsinogen5 ISREs, and significant promoter activity was observed when IRF1, IRF5 or IRF7 was overexpressed (Fig.S3B). Furthermore, the -216 to +15 promoter region of trypsinogen5 was sufficient for responses to IRF1 or IRF7 stimulation (Fig. S3C). Overexpression of IRF2 inhibited IRF1- or IRF7-stimulated promoter activity in a dose-dependent manner (Fig S3D). These data suggest that IRF2 binds to the proximal promoter of trypsinogen5 and inhibits the access of IRF1, IRF5 and IRF7 to ISRE sites in this region.

To confirm this hypothesis, we transfected TGP49 cells, a mouse acinar cell line, with the trypsinogen5 promoter deletion series reporters as well as plasmids expressing IRF1, 5 or 7, and assessed the promoter activities (Fig.2B right). The basal promoter activity was drastically decreased by deleting the -216 to -100 containing two ISREs, a nuclear factor activated T cell (NFAT), and an activator protein-1 (AP-1) binding sites. In contrast to 293T cells, the trypsinogen5 promoter in

TGP49 cells could be activated by exogenously-expressed IRF5 or IRF7 without MyD88 (Fig.3A). The promoter could not be activated by IRF1 even in the presence of MyD88 expression. The regions responsive to IRF5 and IRF7 were confirmed to be ISRE4 (-62 to -59) and ISRE3 (-55 to -49) by site-specific mutation analysis (Fig.2C). The IRF5- and IRF7-dependent promoter activities were significantly ( $p<0.05$ ) enhanced by knocking-down IRF2 with specific siRNA compared to control (scrambled) siRNA (Fig.3A).

To confirm IRF2 binding to the proximal promoter of trypsinogen5 in pancreatic acinar cells *in vivo*, we performed chromatin immunoprecipitation (ChIP) assays in TGP49 cells using specific PCR probes spanning all seven ISREs (-173 to +56) in the trypsinogen5 promoter. Anti-IRF2 antibody (Ab) specifically precipitated the trypsinogen5 promoter, as determined by semi-quantitative PCR (Fig.3B) and real-time PCR (Fig.3C). These results suggest that in WT mice, trypsinogen5 expression in pancreatic acinar cells is repressed by the binding of IRF2 to ISREs in the proximal promoter region. However, in IRF2<sup>-/-</sup> mice, the trypsinogen5 gene is activated because IRF5 and IRF7 can access the ISREs in the absence of IRF2.

IRF5 and IRF7 are critical inducers of the expression of proinflammatory cytokines and type I IFNs, respectively (18,19), and these activities require MyD88. In WT cells, IRF4 inhibits IRF5 function by sequestering MyD88 (18). IRF-2 did not associate with MyD88 (18), but in our study, it did bind to the ISRE-containing region in the trypsinogen5 promoter (Fig.3B,C). Therefore, we postulate that IRF-2 inhibits IRF5 and IRF7 activity by competing with them for binding to ISREs, rather than by sequestering MyD88.

### **Trypsinogen5 is resistant to the trypsin inhibitor Spink3**

Comparison of mouse trypsinogen5 to other mouse and human trypsinogens (Fig.S4) showed that, although the N-terminal activation peptide sequence (NSDDK-I) in trypsinogen5 differs from that in other trypsinogens (DDDDK-I), other important regions, including the triad amino acid sequence, **H-D-S**, required for enzymatic activity, are conserved (10,11). In addition, tryptic activity in cell lysates of 293FT cells overexpressing trypsinogen5 was dramatically enhanced by treatment with enteropeptidase (EP) (Fig.4A,B). The trypsinogen5 inhibitor binding site (DSCDGDS), which prevents premature activation, differed from that found in most trypsinogens (DSCQGDS) (10,11), resembling the inhibitor binding site (DSCQRDS) of the human trypsin inhibitor-resistant PRSS3 enzyme. In addition, the trypsin autocatalytic cleavage site (Q-V) in trypsinogen5 differed from that in other trypsinogens (R-V), suggesting that trypsinogen5 is resistant to both trypsin inhibitors and self-inactivation. Indeed, trypsinogen5 was resistant to inhibition by Spink3, a major endogenous trypsin inhibitor in mice (Fig.4C,D), as well as soy bean trypsin inhibitor (SBTI) (Fig.S5A,B). Analysis of the evolutionary pedigree in Fig.S6 showed that mouse trypsinogen5 is most distant from mPrss1 and mPrss2, just as human PRSS3 is most distant from PRSS1 and PRSS2. Therefore, we believe that mouse trypsinogen5 is a homologue of human PRSS3. Moreover, our data suggest that, in the absence of IRF2, trypsinogen5 is highly expressed and exacerbates pIC-induced pancreatitis due to its inhibitor-resistant nature.

## **Poly(I:C)-induced cell death can be triggered by a TLR3/TRIF-dependent pathway or a RIG-I/MDA5/IPS-1-dependent pathway**

Although trypsinogen5 was up-regulated in untreated IRF2<sup>-/-</sup> mice, only mild inflammation around acinar cells was observed and pancreatitis did not occur. We hypothesize that trypsinogen5 as well as mPrss1, 2, and 3 leaking from dying acinar cells, is activated by proteases such as cathepsin B or enteropeptidase, also released from these cells. These activated trypsins trigger signals to induce the death of many acinar cells, a process of cell death amplification we refer to as the “enhancing loop” of acinar cell death. In this way, the initial death of a few cells induced by pIC can precipitate severe pancreatitis. This idea is supported by a report that the extracellular or intracellular treatment of pancreatic acinar cells with active trypsins causes acinar cell death (20). In this study, the enteropeptidase-cleavage site (-DDDDK-) of rat trypsinogen was replaced with a cleavage site (-RTKR-) recognized by paired basic amino acid cleaving enzyme (PACE). This allowed the rat trypsinogen to be activated intracellularly with the ubiquitously expressed PACE enzyme rather than with enteropeptidase, which is expressed mainly in the duodenum. We created a PACE-trypsinogen5 enzyme, which successfully induced the apoptosis of 293FT cells when overexpressed (Fig.4E,F). These results indicate that proteolytic activation of trypsinogen5 is sufficient to induce for cell death.

Since pIC-dependent pancreatitis in IRF2<sup>-/-</sup> mice can be prevented by inactivating IFNAR1 signaling (Fig.1E), we focused on IFN signaling pathways to identify candidates which might trigger initial cell death following pIC treatment. Indeed, *IRF1*, *IRF7*, *MyD88*, *MDA5*, *RIG-I*, and *TLR3* gene expression were all up-regulated in the pancreas of pIC-IRF2<sup>-/-</sup> mice (Table S2). Because these

proteins are associated with the cell death pathways dependent on TRIF or IPS-1, we examined the effect of IRF2 loss on these well characterized systems (21,22). TRIF binds to receptor-interacting proteins (RIPs) and thereby activates caspase8 via FADD to induce cell death (21), whereas the IPS-1-dependent cell death pathway, which is triggered by MDA5 or RIG-I, is reported to activate caspase9 via the mitochondrial pathway dependent on Apaf-1 and cytochrome c (22). We confirmed that 293FT cells transfected with TRIF-expressing plasmid underwent apoptosis, as shown by staining with FITC-labeled annexin V (Fig.5B). Next, we employed the MTT viability assay to quantify the extent of cell death induced by IFN-related molecules in the presence or absence of pIC and IFN $\alpha$ . Exogenous overexpression of IPS-1 or TRIF significantly enhanced the death of pIC- and IFN-treated 293FT cells, and the death-inducing effects of MDA5 and RIG-I were enhanced by co-transfection with IPS-1 (Fig.5A). These results suggest the existence of at least two pIC-dependent cell death pathways: one TLR/TRIF-dependent, and one RIG-I/MDA5/IPS-1-dependent.

We used real-time PCR to examine the induction of TLR3, RIG-I and MDA5 mRNAs in pIC-treated WT, IRF2<sup>-/-</sup>, and IRF2<sup>-/-</sup>/IFNAR1<sup>-/-</sup> mice. The levels of all three mRNAs were induced by nearly 100-fold in both pIC-WT and pIC-IRF2<sup>-/-</sup> mice, and these increases were abolished by deletion of IFNAR1 (Fig.5C-E). As shown in Fig.6 and Table S3, the IFN signal activation triggered by pIC is essential to initiate the TLR/TRIF- and RIG-I/MDA5/IPS-1-dependent acinar cell death, but is not sufficient to cause pancreatitis. The elevation of trypsinogen5 expression mediated by abolishing IRF2, is also necessary for enhancing the cell death leading to the lethal pancreatitis.

### **Activation mechanisms of mouse trypsinogen5 and human PRSS3**

Trypsinogens (including trypsinogen5) can be activated in pancreatic acinar cells, or in other cells or tissues by enteropeptidase expressed in non-duodenal cells (23), such as in keratinocytes and oral carcinoma cells (24,25). It is possible that keratinocyte-expressed enteropeptidase activates the trypsinogen5 expressed in skin (Fig.S3A), promoting age-dependent skin inflammation in IRF-2<sup>-/-</sup> mice (4). Another possibility could be that proteases in addition to enteropeptidase can cleave pancreatic trypsinogen5. We have confirmed that cathepsin B, whose expression was elevated in IRF2<sup>-/-</sup> mice, can activate trypsinogen5 *in vitro* (Fig. S5C). The last possibility is that autocatalytic cleavage of trypsinogen, usually restricted under steady-state conditions, is accelerated in response to a chemical stress or viral infection. Indeed, the auto-activation of trypsinogen is reportedly accelerated in low pH or by Ca<sup>2+</sup> *in vitro* (26).

In conclusion, this study has identified important genes associated with IRF2 functions in mice. Our results suggest that IRF2 influences the expression of mouse trypsinogen5, whose human counterpart is PRSS3. Our data should therefore help to elucidate new IRF functions in humans.

## **Materials and Methods**

### **Mice**

IRF1<sup>-/-</sup>, and IRF2<sup>-/-</sup> mice have been described (3). IFN- $\alpha/\beta$  receptor 1 (IFNAR1)<sup>-/-</sup> mice were purchased from B&K Universal (8). TRIF<sup>-/-</sup> mice have been described (9). IRF-2<sup>-/-</sup>/IFNAR1<sup>-/-</sup>, IRF-2<sup>-/-</sup>/IRF1<sup>-/-</sup>, and IRF-2<sup>-/-</sup>/TRIF<sup>-/-</sup> double mutant mice were generated by crossing IRF-2<sup>+/-</sup>, with IFNAR1<sup>-/-</sup>, IRF1<sup>-/-</sup>, and TRIF<sup>-/-</sup> mice, respectively. All mice were maintained under specific pathogen-free conditions and used at 6-12 week of age. All experiments were performed according to institutional guidelines.

### **Cells**

Human embryonic kidney (HEK) 293T and 293FT (Invitrogen) cells, and HeLa cells were cultured in Dulbecco's modified Eagle's medium supplemented with 10% fetal bovine serum. Mouse pancreatic acinar TGP49 cells were cultured in 1:1 mixture of Dulbecco's modified Eagle's medium and Ham's F12 medium supplemented with 10% fetal bovine serum.

### **Histological analysis**

The pancreas tissues were fixed overnight in 10% formalin, embedded in paraffin, sectioned, and stained with hematoxylin (0.4%) and eosin (0.5%) for light microscopic analysis. For electron microscopic analysis, the tissues were fixed in 2.5% glutaraldehyde solution buffered to pH 7.4 with 0.1M phosphate buffer for 4h at 4°C. Postfixation was performed with 2% osmium tetroxide solution buffered to pH 7.4 with the same buffer for 2h at 4°C, and they were embedded, sectioned, and doubly stained with uranyl acetate and lead nitrate.

## **Microarrays**

Total RNAs from the pancreas of wild type and IRF2<sup>-/-</sup> mice aged 6 weeks, harvested 3h after no injection or a peritoneal injection with 250 µg poly(I:C), were used in the array studies. The quality of the RNA was assessed with an Agilent 2100 Bioanalyzer, and samples of 100 ng total RNA were reverse transcribed and then amplified *in vitro* transcription according to Affymetrix standard protocols. The mouse Affymetrix GeneChip Mouse Gene 1.0 ST Array was used in all hybridizations. These arrays contain probes representing transcripts for 28,815 mouse gene entities. Microarray data were analyzed using the Affymetrix Expression Console Software, and Gene Spring GX, whereas differentially expressed genes were identified with annotation.

## **Real-time RT-PCR**

Total RNA was prepared from tissues using the acid phenol-guanidinium thiocyanate method, after immersing the tissues for more than overnight in RNA Later solution (Ambion). Reverse transcription was conducted for 60min at 46°C from 200 ng of purified total RNA using Superscript III (Invitrogen), followed by 45 cycles of PCR (15s denaturation at 95°C, 25s annealing at 55°C and 15s extension at 72°C). A SYBR Green PCR kit (Qiagen) was used to monitor the PCR products on the LightCycler 1.5 and real-time PCR detection system (Roche). Primers designed for respective genes are listed in Table S5.

## **Plasmid constructs**

The cDNA encoding human IRF1, IRF7, and IPS-1 were generated from total RNA prepared from 293T cells by RT-PCR, using KOD-FX DNA polymerase (TOYOBO). The human

MDA5, RIG-I, and TLR3 cDNAs were generated from total RNA prepared from THP-1 (a human leukemia cell line), or HeLa cells by RT-PCR. The mouse Trypsinogen5, Prss1, and Spink3 cDNAs were made from total RNA prepared from WT mouse pancreas by PCR. All constructs generated by PCR were confirmed by DNA sequencing. The pTrypsinogen5-Luc reporter plasmid was constructed by inserting the promoter region (-1063 to +15) of the mouse trypsinogen 5 gene by PCR into the pGL2-Basic vector. A series of deletion mutants were made using proper restriction enzymes (NcoI at -833; SpeI at -579; ScaI, at -386; PvuII at -216), and a specific primer for -100 site. The promoter region (-216 to +15) of the mouse trypsinogen 5 gene was used to introduce point mutations into the ISREs. The point mutations of the ISRE3 (-55 to-49, ATTGAAA→GTTTGCG), ISRE4 (-62 to-59, TTTC→CGCA), and ISRE5 (-84 to-78, AATGAAA→GATTGCG) were introduced by overlap PCR mutagenesis. All constructs generated by PCR were confirmed by DNA sequencing.

The PACE-Trypsinogen5 was constructed replacing the activation peptide (-NSDDK-) of the mouse trypsinogen5 cDNA with the PACE recognition peptide (-RTKR-), by overlap PCR mutagenesis.

### **Luciferase reporter assay**

293T cells ( $1 \times 10^5$ /well) were plated in 24-well plates, and transfected 24h later with 200 ng of the firefly luciferase reporter plasmid pTrypsinogen5-Luc, using FuGENE6 (Roche), along with each expression vector (20 ng unless otherwise stated) as indicated. In all cases, cells were transfected with 20 ng pRL-TK (thymidine kinase promoter-driven Renilla luciferase reporter gene, Promega), to normalize the transfection efficiency. TGP49 cells ( $1 \times 10^5$ /well) were plated in 12-well

plates, and transfected 24h later with 1  $\mu\text{g}$  of the firefly luciferase reporter plasmid pTrypsinogen5-Luc, using Lipofectamine 2000 (Invitrogen), along with each expression vector (100 ng unless otherwise stated) as indicated. In all cases, cells were transfected with 20 ng pRL-RSV (RSV promoter-driven Renilla luciferase reporter gene). At 26h post-transfection, the luciferase activity was determined with the dual luciferase assay system. The mouse IRF2-specific and control siRNAs were purchased from Santa Cruz.

### **Chromatin immunoprecipitation (ChIP)**

The nuclear extracts from TGP49 cells were subjected to DNA-protein cross-linking with 1% formaldehyde for 5min. After extensive washing, the samples were suspended in 500  $\mu\text{l}$  of 150 mM NaCl, 25 mM Tris, pH 7.5, 5 mM EDTA, 1% Triton X-100, 0.1% SDS, and 0.5% deoxycholate, and were sonicated. After centrifugation at 14,000 rpm for 10 min at 4°C, the supernatants were immunoprecipitated with 0.5  $\mu\text{g}$  anti-IRF2 antibody, or the corresponding IgG (Sigma) (as a control), and Protein A Sepharose4B Fast Flow beads. The amounts of precipitated DNA were quantified by PCR, using a pair of mouse Trypsinogen5 promoter-specific primers, and Angiotensinogen (Agt) exon2-specific primers (Materials and Methods in SI).

### **Trypsin activity assay**

Trypsin activity was monitored by the amount of released p-nitroaniline (pNA) from a specific substrate, measuring spectrophotometric units at 405 nm ( $A_{405}$ ) (Trypsin activity assay kit of BioVision). Cell lysates prepared at 48h post-transfection of the indicated expression plasmids were used with or without enteropeptidase (light chain, porcine of GenScript).

## Cell death assay

Pancreatic tissues were used in the TUNEL assay. Briefly, tissue sections were incubated with 20 µg/ml proteinase K for 20 min, followed by inhibition of endogenous peroxidase by incubation with 2 % H<sub>2</sub>O<sub>2</sub> for 7 min. TdT (GIBCO-BRL) and biotinylated dUTP (Roche) in TdT buffer were added to the sections and incubated in a humid atmosphere at 37°C for 90 min after immersion in TdT buffer. The reaction was terminated by transferring the slides to TB buffer (300 mM NaCl, 30 mM Na citrate) for 30 min. The sections were covered with 10% rabbit serum for 10 min and then with the avidin-biotin peroxidase complex for 30 min. Finally, DAB was used as the chromogen. To detect the apoptotic cells, FITC-conjugated Annexin V (BioVision) was used according to the manufacturer's instruction. MTT (ICN) assay to assess living cells was performed according to the manufacturer's instruction.

## **Acknowledgements**

This work was supported by Grants-in-Aid from the Ministry of Education, Culture, Sports, Science and Technology of Japan (22659092), and by the Global Center of Excellence Program at Nagasaki University (<http://www.tm.nagasaki-u.ac.jp/gcoe/>).

## References

- 1: Savitsky D, Tamura T, Yanai H, Taniguchi T (2010) Regulation of immunity and oncogenesis by the IRF transcription factor family. *Cancer Immunol Immunother* 59:489-510.
- 2: Kawai T, Akira S (2011) Toll-like receptors and their crosstalk with other innate receptors in infection and immunity. *Immunity* 34:637-650.
- 3: Matsuyama T, Kimura T, Kitagawa M, Pfeffer K, Kawakami T, et al (1993) Targeted disruption of IRF-1 or IRF-2 results in abnormal type I IFN gene induction and aberrant lymphocyte development. *Cell* 75:83-97.
- 4: Hida S, Ogasawara K, Sato K, Abe M, Takayanagi H, et al (2000) CD8(+) T cell-mediated skin disease in mice lacking IRF-2, the transcriptional attenuator of interferon-alpha/beta signaling. *Immunity* 13:643-655.
- 5: Lampel M, Kern H-F (1977) Acute interstitial pancreatitis in the rat induced by excessive doses of a pancreatic secretagogue. *Virchows Arch A Pathol Anat Histol.* 373:97-117.
- 6: Mashima H, Sato T, Horie Y, Nakagawa Y, Kojima I, et al (2011) Interferon Regulatory Factor-2 Regulates Exocytosis Mechanisms Mediated by SNAREs in Pancreatic Acinar Cells. *Gastroenterology* 141:1102-1113.
- 7: Gerke V, Creutz C-E, Moss S-E. (2005) Annexins: linking Ca<sup>2+</sup> signalling to membrane dynamics. *Nat Rev Mol Cell Biol* 6:449-461.
- 8: Hwang SY, Hertzog PJ, Holland KA, Sumarsono SH, Tymms MJ, et al (1995) A null mutation in the gene encoding a type I interferon receptor component eliminates antiproliferative and antiviral responses to interferons alpha and beta and alters macrophage responses. *Proc Natl Acad Sci USA* 92:11284-11288.
- 9: Yamamoto M, Sato S, Hemmi H, Hoshino K, Kaisho T, et al (2003) Role of adaptor TRIF in the MyD88-independent toll-like receptor signaling pathway. *Science* 301:640-643.
- 10: Chen J-M, Férec C (2009) Chronic pancreatitis: genetics and pathogenesis. *Annu Rev Genomics Hum Genet* 10:63-87.
- 11: Whitcomb D-C (2010) Genetic aspects of pancreatitis. *Annu Rev Med.* 61:413-424.

- 12: Spicuglia S, Pekowska A, Zacarias-Cabeza J, Ferrier P (2010) Epigenetic control of Tcrb gene rearrangement. *Semin Immunol.* 22:330-336.
- 13: Rowen L, Williams E, Glusman G, Linardopoulou E, Friedman C, et al (2005) Interchromosomal segmental duplications explain the unusual structure of PRSS3, the gene for an inhibitor-resistant trypsinogen. *Mol Biol Evol* 22:1712-1720.
- 14: Figarella C, Miszczuk-Jamska B, Barrett A-J (1988) Possible lysosomal activation of pancreatic zymogens. Activation of both human trypsinogens by cathepsin B and spontaneous acid. Activation of human trypsinogen 1. *Biol Chem Hoppe Seyler* 369 Suppl:293-298.
- 15: Halangk W, Lerch M-M, Brandt-Nedelev B, Roth W, Ruthenbueger M, et al (2000) Role of cathepsin B in intracellular trypsinogen activation and the onset of acute pancreatitis. *J Clin Invest* 106:773-781.
- 16: Meister T, Niehues R, Hahn D, Domschke W, Sandler M, et al (2010) Missorting of cathepsin B into the secretory compartment of CI-MPR/IGFII-deficient mice does not induce spontaneous trypsinogen activation but leads to enhanced trypsin activity during experimental pancreatitis--without affecting disease severity. *J Physiol Pharmacol* 61:565-575.
- 17: Hashimoto D, Ohmuraya M, Hirota M, Yamamoto A, Suyama K, et al (2008) Involvement of autophagy in trypsinogen activation within the pancreatic acinar cells. *J Cell Biol* 181:1065-1072.
- 18: Negishi H, Ohba Y, Yanai H, Takaoka A, Honma K, et al (2005) Negative regulation of Toll-like-receptor signaling by IRF-4. *Proc Natl Acad Sci USA* 102:15989-15994.
- 19: Honda K, Ohba Y, Yanai H, Negishi H, Mizutani T, et al (2005) Spatiotemporal regulation of MyD88-IRF-7 signalling for robust type-I interferon induction. *Nature* 434:1035-1040.
- 20: Ji B, Gaiser S, Chen X, Ernst S-A, Logsdon C-D. Intracellular trypsin induces pancreatic acinar cell death but not NF-kappaB activation (2009) *J Biol Chem* 284:17488-17498.
- 21: Kaiser W-J, Offermann M-K (2005) Apoptosis induced by the toll-like receptor adaptor TRIF is dependent on its receptor interacting protein homotypic interaction motif. *J Immunol* 174:4942-4952.
- 22: Lei Y, Moore C-B, Liesman R-M, O'Connor B-P, Bergstralh D-T, et al (2009) MAVS-mediated apoptosis and its inhibition by viral proteins. *PLoS One* 4:e5466.

- 23: Yahagi N, Ichinose M, Matsushima M, Matsubara Y, Miki K, et al (1996) Complementary DNA cloning and sequencing of rat enteropeptidase and tissue distribution of its mRNA. *Biochem Biophys Res Commun* 219:806-812.
- 24: Nakanishi J, Yamamoto M, Koyama J, Sato J, Hibino T. Keratinocytes synthesize enteropeptidase and multiple forms of trypsinogen during terminal differentiation. *J Invest Dermatol* 130:944-952.
- 25: Vilen S-T, Nyberg P, Hukkanen M, Sutinen M, Ylipalosaari M, et al (2008) Intracellular co-localization of trypsin-2 and matrix metalloprotease-9: possible proteolytic cascade of trypsin-2, MMP-9 and enterokinase in carcinoma. *Exp Cell Res* 314:914-926.
- 26: Chen J-M, Kukor Z, Le Maréchal C, Tóth M, Tsakiris L, et al (2003) Evolution of trypsinogen activation peptides. *Mol Biol Evol* 20:1767-1777.

## Legends for Figures

**Fig.1 IRF2 deficiency induces sensitivity to poly(I:C) and pancreatitis.** **A.** Survival curve after pIC challenge. WT and IRF2-deficient (IRF2<sup>-/-</sup>) mice were induced by intraperitoneal pIC challenge (250 µg). All the IRF2<sup>-/-</sup> mice were deceased within a week, compared to WT mice. **B.** Following pIC stimulation, many cells were TUNEL-positive, indicating apoptosis and severe acute pancreatitis, in IRF2<sup>-/-</sup> mice. Hematoxylin and eosin (HE) staining (**C**) and electron microscopic observation (**D**) were done to examine the pancreas histologically in wild-type, IRF2<sup>-/-</sup>, and the double KO mice (IRF-2<sup>-/-</sup>/IFNARI<sup>-/-</sup>, IRF-2<sup>-/-</sup>/IRF1<sup>-/-</sup>, and IRF-2<sup>-/-</sup>/TRIF<sup>-/-</sup>). **E.** To assess the pancreatitis, we monitored the serum amylase level with (+) and without (-) pIC challenge.

**Fig.2 Trypsinogen5 is highly expressed in IRF2-deficient mice.** **A.** The IRF2<sup>-/-</sup>, or wild type mice with or without peritoneal injection of pIC were sacrificed, and the amounts of mRNA from the pancreas were systemically compared using Affymerix 28,815 gene probes. The points furthest from the diagonal indicate transcripts showing the greatest difference between the WT and IRF2<sup>-/-</sup>. Points 1 and 2: Trypsinogen5 with different probes; 3: α-2-HS-glycoprotein (Ahsg); 4: annexin A10 (Anxa10); 5: fetuin-β (Fetub); 6: 3-hydroxy-3-methylglutaryl-CoenzymeA synthase2 (Hmgcs2, HMG-CoA synthase); 7: immunoglobulin kappa chain variable8 (Igf-V8); 8: unknown; 9: carbonic anhydrase 3 (Car3). **B.** A series of deletion mutants of trypsinogen5 proximal promoter region (-216 to +15) were placed upstream of a luciferase reporter gene (1 µg), and were analysed for transcriptional activity in mouse pancreatic acinar cells using a dual luciferase assay, at 24h

posttransfection in combination with expressions vectors (100 ng) expressing IRF5 or IRF7 or a control vector. The basal luciferase activity of each deletion, measured relative to the -216 to +15 region, and the responses to IRF5 and IRF7 expression vectors were shown as fold-increase to the control vector. The TATA box, ISRE core, NFAT-, and AP-1-binding sites are indicated. \* $p < 0.05$  vs. the -216 to +15 region. **C.** Point mutations were introduced in each ISRE site (indicated by x) of the trypsinogen5 promoters as described under Materials and Methods. The promoter activity of each mutant trypsinogen5 was determined with the dual luciferase assay system. \* $p < 0.05$  vs. wild type.

**Fig. 3 IRF-2 binds to the promoter region of trypsinogen5 gene.** **A.** The effects of siRNAs (3  $\mu$ g) specific to IRF2 or a control scrambled sequence on transcriptional activity of the -216 to +15 luciferase reporter in TGP49 acinar cells were measured. \* $p < 0.05$  vs. the control siRNA. **B.** Chromatin immunoprecipitation (ChIP) assay was done using TGP49 acinar cells with the IRF2-specific antibody (5  $\mu$ g), or the same amount of control non-specific IgG. The precipitated chromatin fragments were detected by PCR with a trypsinogen5 promoter-specific primer set at 35 cycles, or a negative control primer set for angiotensinogen (Agt) exon2 at 30 (upper panel) and 35 (lower panel) cycles. The input before precipitation indicates the predicted size (Trp5:289bp, Agt:221bp) of the PCR product. **C.** The ChIP assay done in **B** was quantitatively measured using real-time PCR method with the same primers. The relative amounts to  $\beta$ -actin were calculated, and the amounts of chromatin fragments precipitated with the anti-IRF2 antibody were shown relative to those with the nonspecific control antibody (IgG). \* $p < 0.01$  vs. the control IgG.

**Fig.4 Trypsinogen activity is activated by proteolytic cleavage. A, B.** A full-length mouse trypsinogen5 cDNA from the mouse pancreas was cloned into pcDNA3 (Invitrogen), and expressed in 293T cells. The indicated amounts cell lysates (2 ~ 8  $\mu$ l of 5  $\mu$ g/ $\mu$ l lysates) were mixed with a trypsin specific substrate (BioVision), in the presence or absence of added enteropeptidase (EP). Tryptic activity was monitored by the amount of released pNA measuring spectrophotometric units ( $A_{405}$ ). **C, D.** The effects of Spink3 were examined by adding the cell lysates expressing Spink3, a major intrinsic trypsin inhibitor in the mouse pancreas, to the lysates expressing trypsinogen5 (**C**), or mouse Prss1 (**D**). **E.** The DNA sequence encoding the activation peptide in the trypsinogen5 expression vector was replaced with sequences encoding a PACE cleavage site (-RTKR-) so that the tryptic activity is activated by ubiquitously expressed PACE protease. **F.** The 293FT cells transfected with the PACE-trypsinogen5 or control vector were stained with FITC-labeled annexin V to detect apoptosis.

**Fig.5 Poly(I:C) and IFN $\alpha$  treatment induces cell death through different pathways. A.** Viabilities of the 293FT cells transfected with the indicated expression plasmids in the presence or absence of pIC (5  $\mu$ g/ml) and IFN $\alpha$  (50 ng/ml) for 44h were quantified with MTT assay. The values represent the average of at least three separate experiments with standard deviation shown by error bars. TRIF, and IPS-1 with MDA5 or RIG-I induced significant (\* $p < 0.02$ ) cell death in response to pIC and IFN $\alpha$ . **B.** The 293FT cells transfected with TRIF expression vector or vector alone were stained with FITC-labeled annexin V to detect apoptosis. The mRNA expression levels of TLR3 (**C**),

RIG-I (**D**), and MDA5 (**E**) were measured using real-time PCR with (+) or without (-) intraperitoneal pIC injection (250  $\mu$ g). The mRNAs prepared from the pancreas, liver, and spleen of wild type (WT), IRF2<sup>-/-</sup>, IRF2<sup>-/-</sup>/IFNAR1<sup>-/-</sup> mice were converted into cDNA, and the amount of cDNA was determined by real-time PCR with specific primers listed in Supplemental Table 5. The values represent the average of at least two mice with standard deviation shown by error bars. \*p<0.05 vs. the IRF2<sup>-/-</sup> mice.

Fig.1

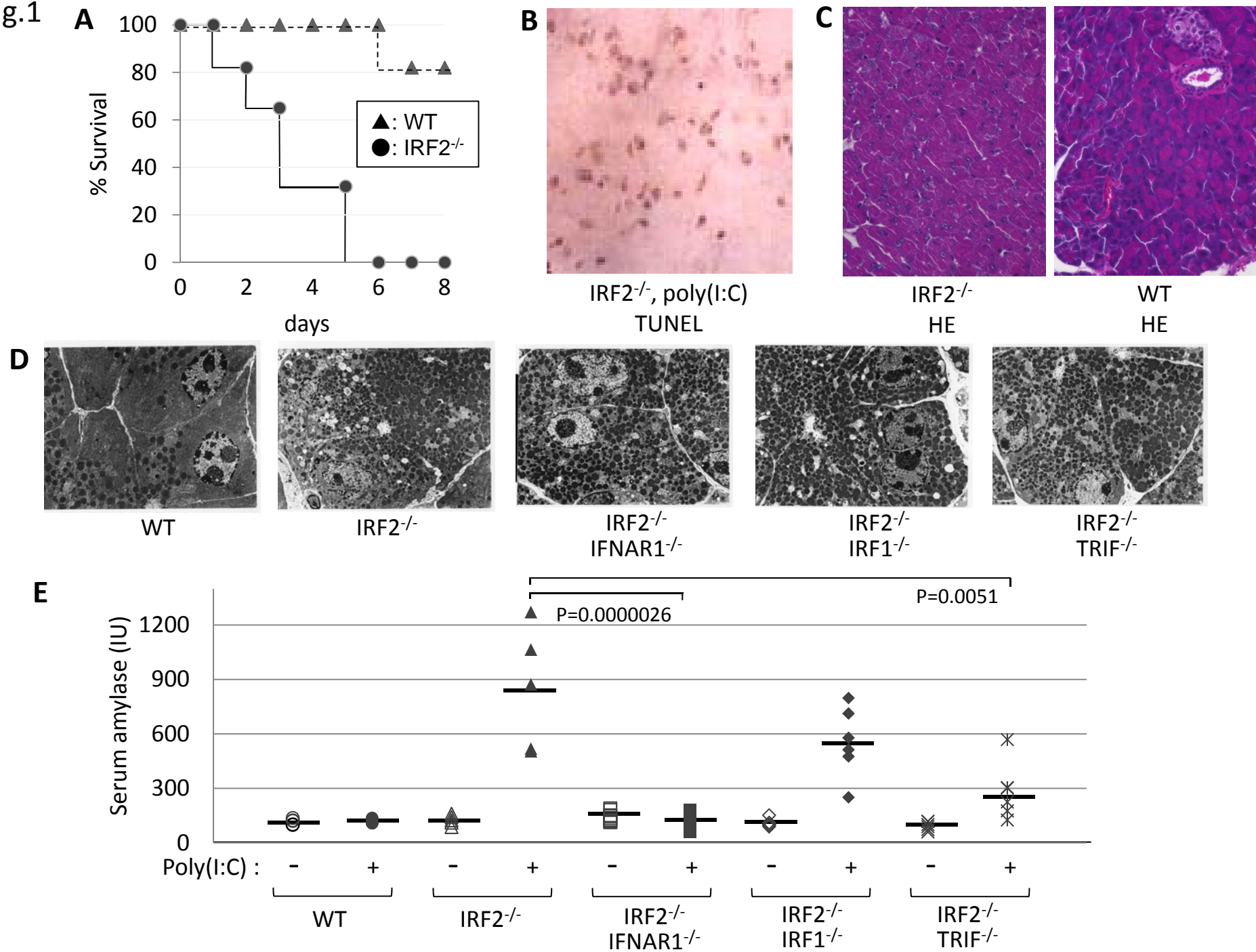


Fig.2

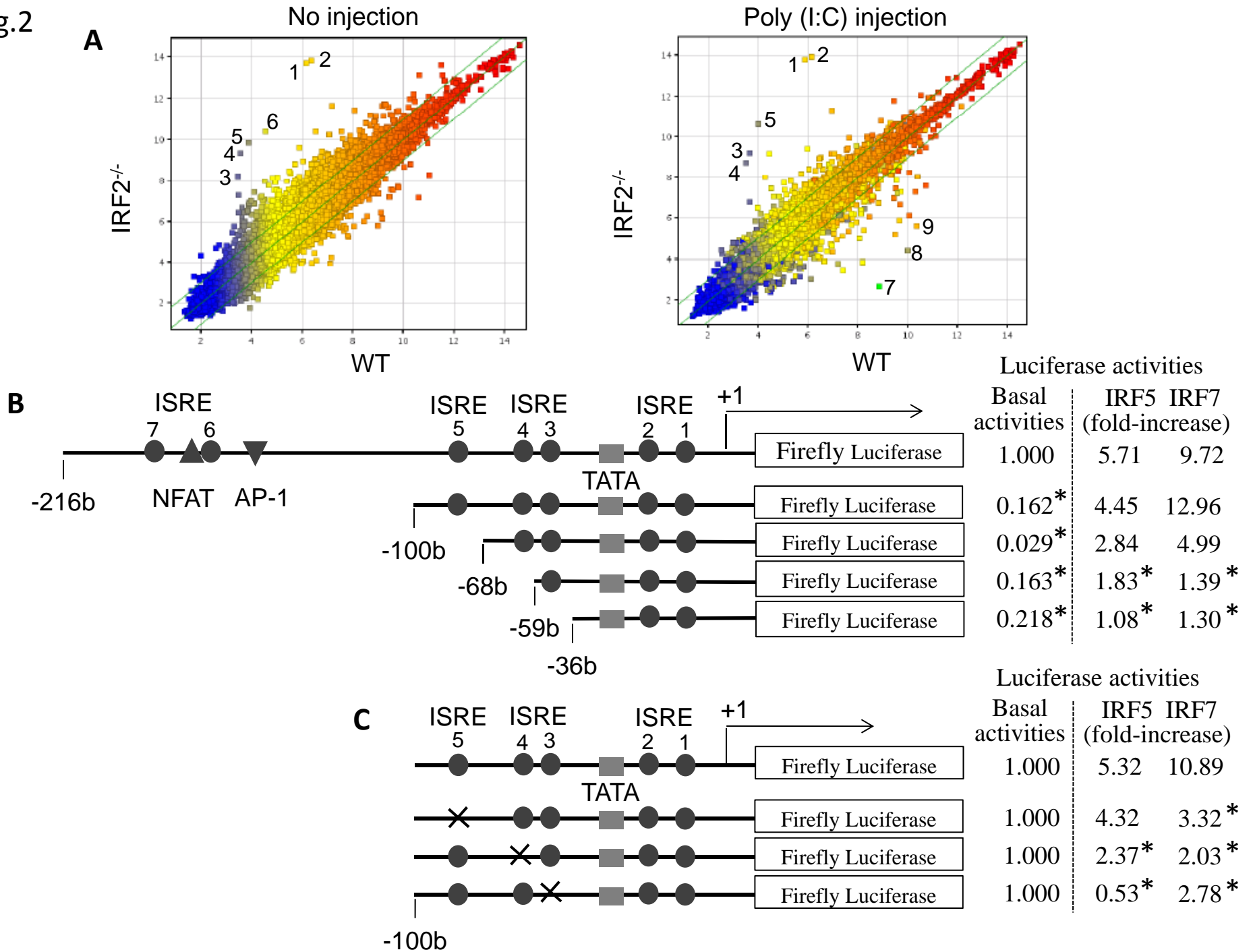


Fig.3

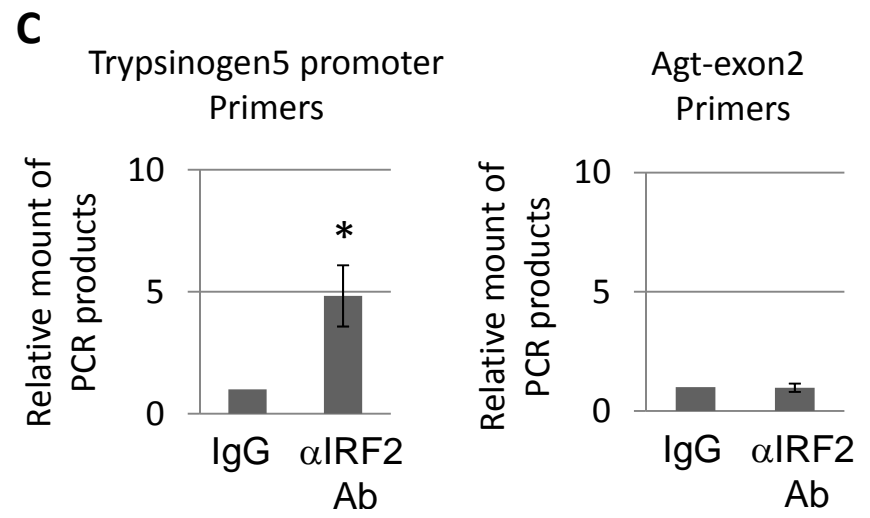
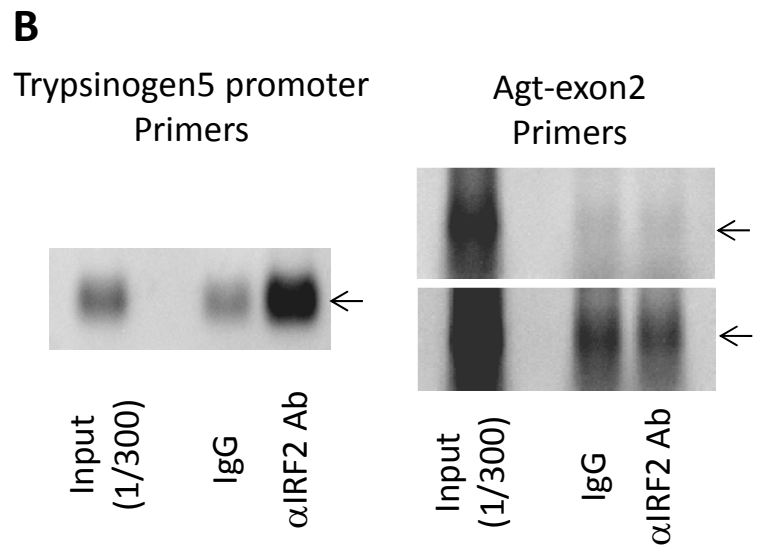
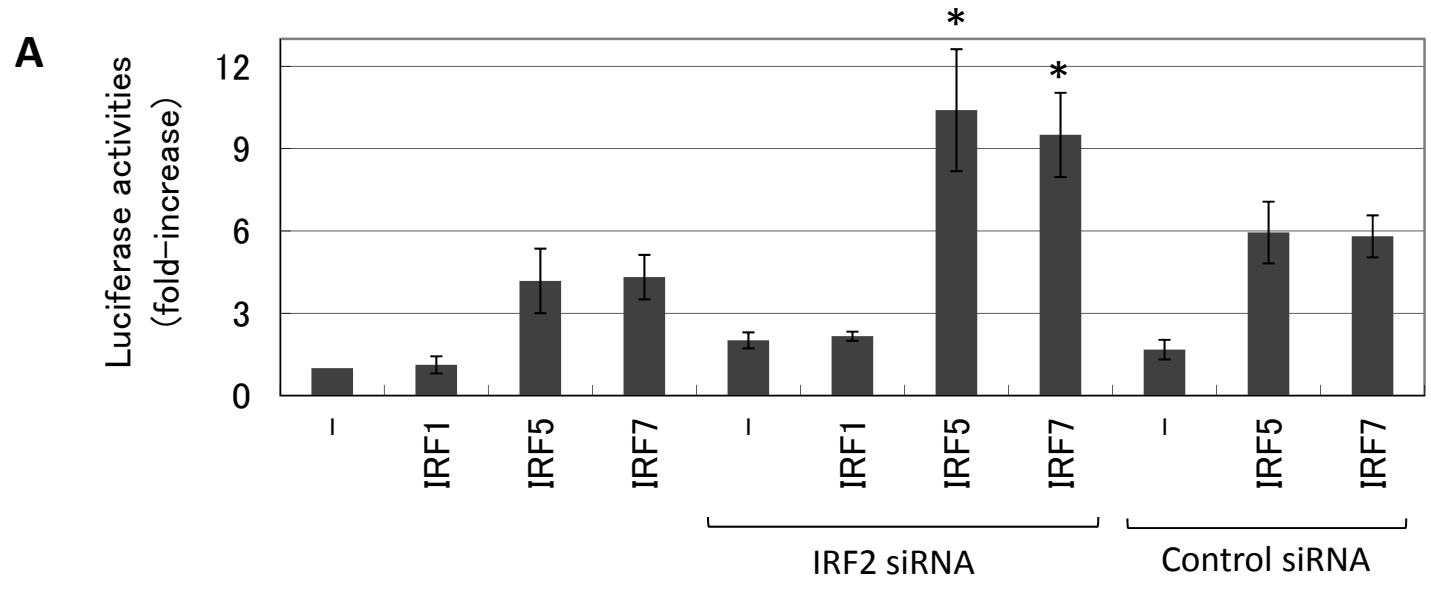


Fig.4

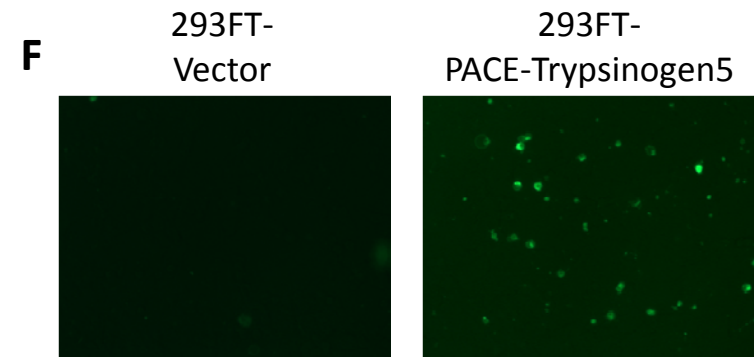
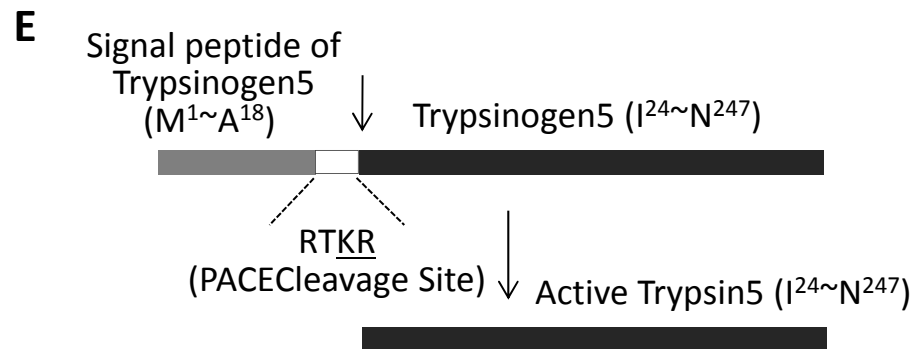
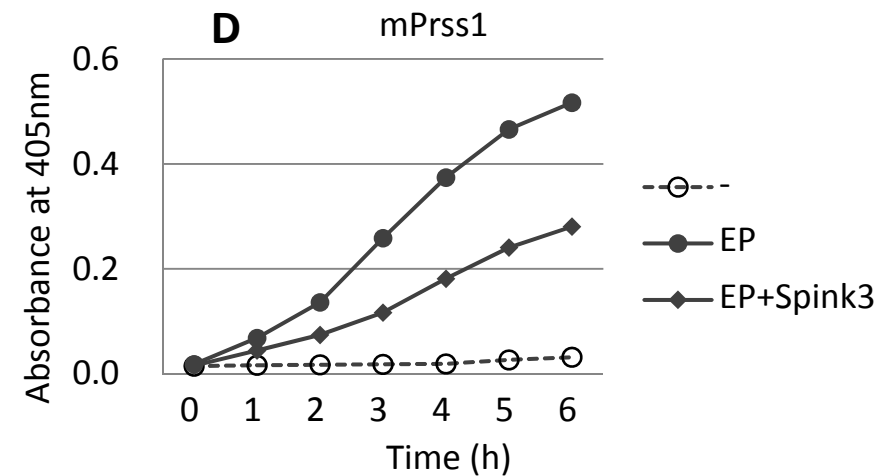
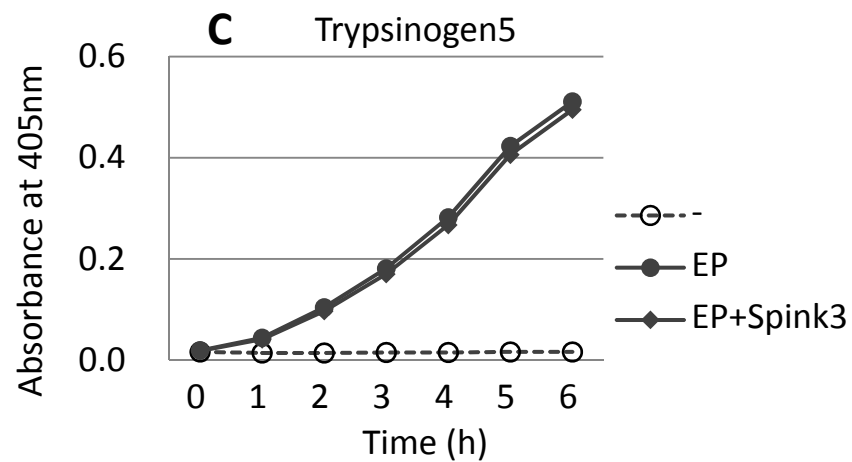
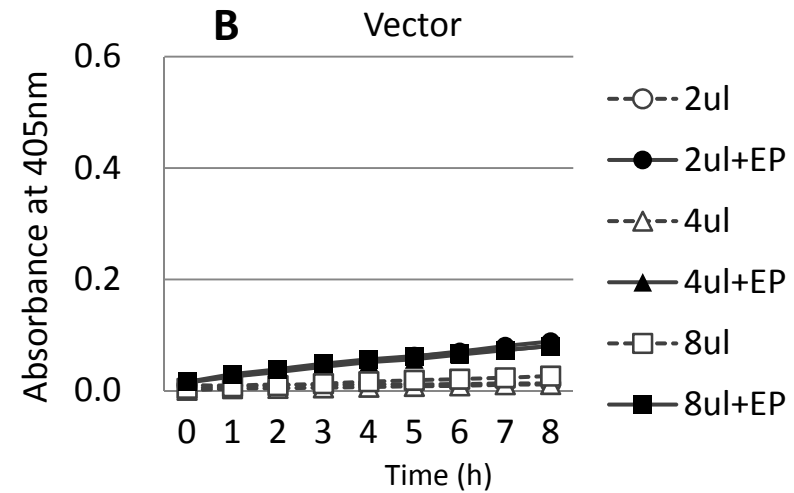
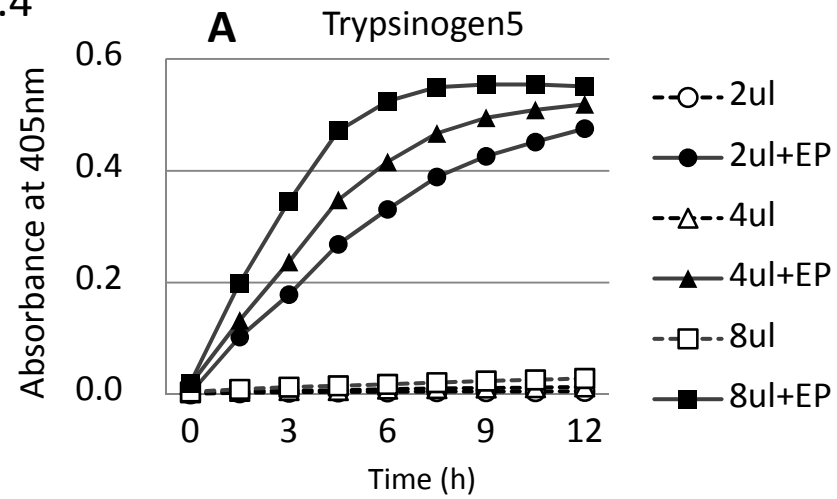
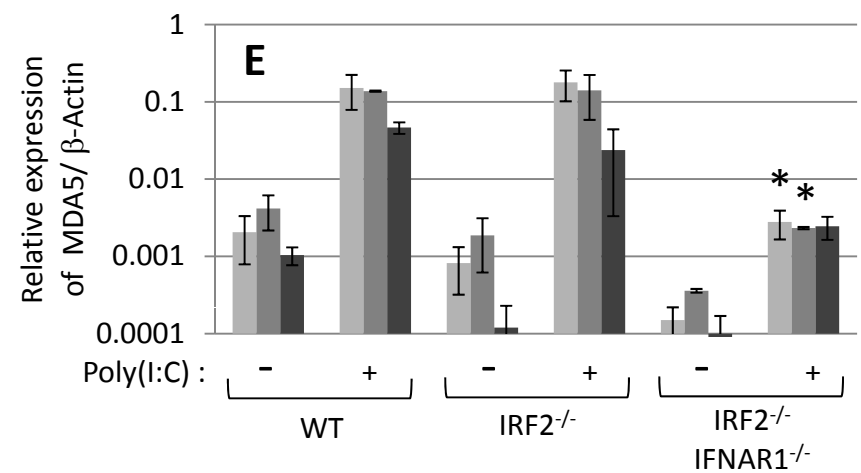
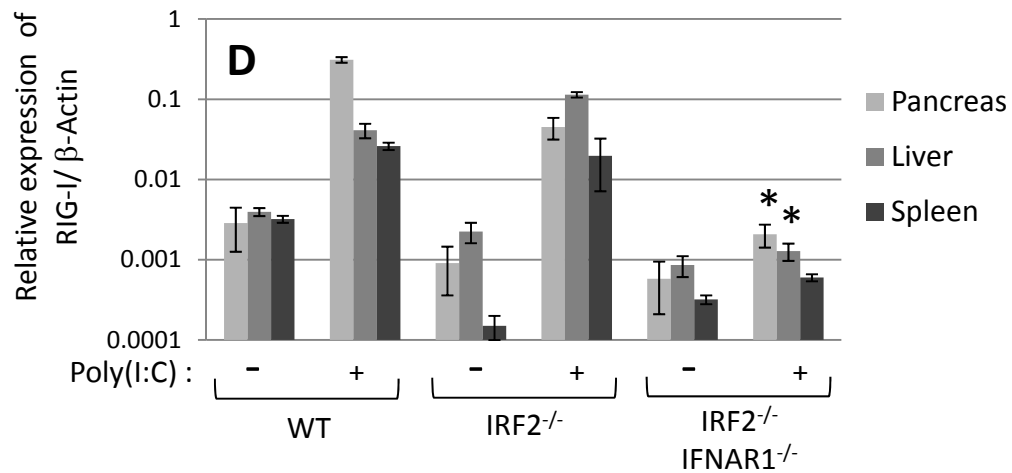
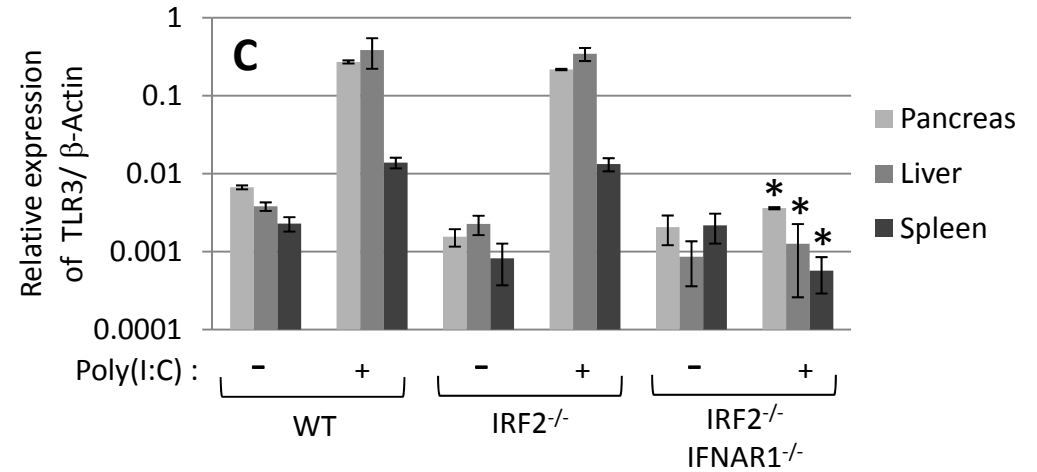
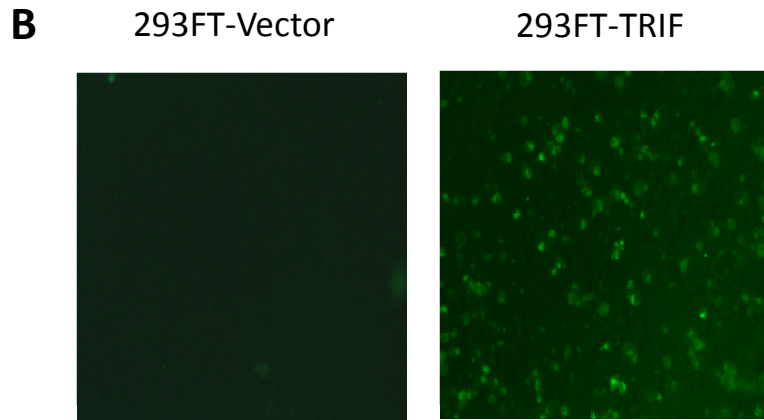
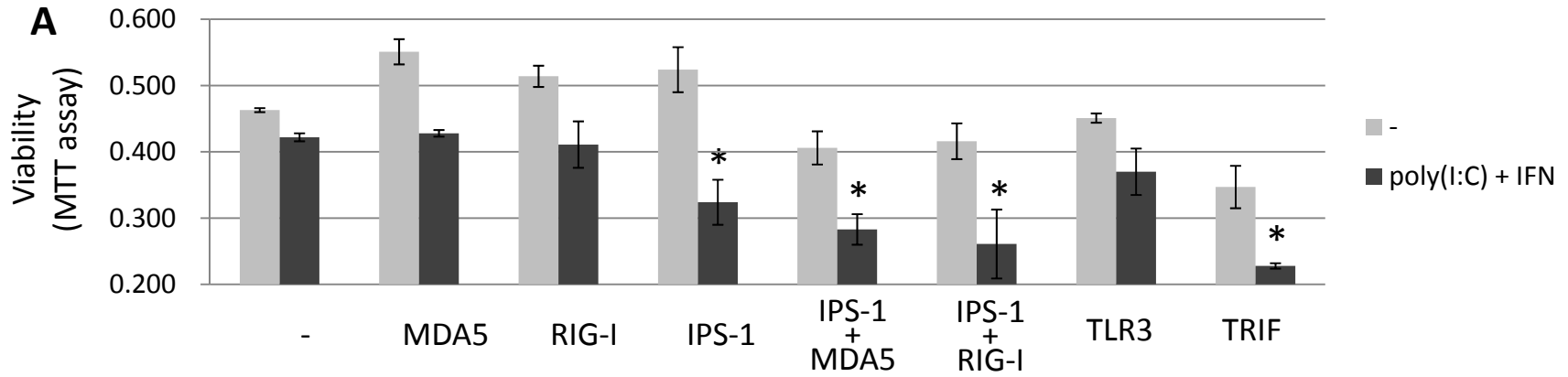


Fig.5



**Table 1.** Expressions of relevant genes to Pancreatitis

<b>Genes</b>	<b>WT (-)</b>	<b>WT (poly I:C)</b>	<b>IRF2<sup>-/-</sup> (-)</b>		<b>IRF2<sup>-/-</sup> (poly I:C)</b>
Prss1 (T16, Trypsin1)	11,161	13,863	10,388		13,788
Prss2 (T20, Trypsin 2)	16,041	15,661	15,857		15,494
<b>Prss3 (T11, Trypsin 3)</b>	1,155	1,131	3,059	↑	2,395
<b>Trypsinogen5 (T4, 1810009J06Rik)</b>	<b>70</b>	<b>57</b>	<b>13,514</b>	↑	<b>14,287</b>
<b>Chymotrypsin C (Ctrc)</b>	545	368	87	↓	119
Chymotrypsinogen B1 (Ctrb1)	19,417	18,772	20,457		19,919
Amylase2-2, pancreatic (Amy2b)	19,101	18,488	17,092		18,261
Calcium-sensing receptor (Casr)	37	37	30		26
Cystic fibrosis membrane conductance regulator (Cftr)	7	6	11		8
<b>Cathepsin B (Ctsb)</b>	349	443	848	↑	794
Serine protease inhibitor, Kazal-type3 (Spink3)	4,716	3,957	7,497		7,774
<b>Inter α-trypsin inhibitor, heavy chain4 (Itih4)</b>	375	212	78	↓	71
<b>Galanin (Gal)</b>	879	1057	213	↓	71

The levels of gene expressions in the pancreas are shown in Affymetrix unit.

## Supporting Information

### Materials and Methods

#### Reagents

Cathepsin B (from bovine spleen) was purchased from MERCK, and N-(p-Tosyl)-GPK-pNA and soy bean trypsin inhibitor (SBTI) were from Sigma.

#### Primers used for Real-time PCR

The mouse  $\beta$ -Actin primers (Forward: 5'-TGGAATCCTGTGGCATCCATGAAAC-3', Reverse: 5'-TAAAACGCAGCTCAGTAACAGTCCG-3'), Trypsinogen5 primers (Forward: 5'-ATTGAAGTCACCTGCCATCC -3', Reverse: 5'-AGGACAGGAGCTTCCAGACA-3'), TLR3 primers (Forward: 5'-TTGTCTTCTGCACGAACCTG-3', Reverse: 5'-CCCGTTCCCAACTTTGTAGA-3'), RIG-I primers (Forward: 5'-TTGCTGAGTGCAATCTCGTC-3', Reverse: 5'-GTATGCGGTGAACCGTCTTT-3'), and MDA5 primers (Forward: 5'-TGTCTTGGACACTTGCTTCG-3', Reverse: 5'-GGCCTCTGTCTCCAGACTTG-3'), were used for real-time PCR.

#### Primers used for ChIP assay

The mouse IRF2 promoter-specific primers (Forward: 5'-CCGGGGGAAACAATGATGTGGAAAC-3', Reverse: 5'-AGCAGCTCCCAGAAAAGTGA-3'), and Angiotensinogen (Agt) exon2-specific primers (Forward: 5'-CACCCCTGCTACAGTCCATT-3', Reverse: 5'-CAGACATGACTGGGGGAGGT-3'), were used for ChIP assay.

## Reference

1: Bhandari M, Thomas AC, Hussey D-J, Li X, Jaya SP, et al (2010) Galanin mediates the pathogenesis of cerulein-induced acute pancreatitis in the mouse. *Pancreas* 39:182-187.

## Legends for Figures

**Supplemental Fig. S1** Resistance of IRF-2<sup>-/-</sup> mice to cerulein-induced pancreatitis. Wild-type or IRF-2<sup>-/-</sup> mice were injected intraperitoneally with 50 µg/kg Cerulein 6 times at hourly intervals. One hour after the last injection, the pancreas was subjected to electron microscopic analysis (**A**), and their serum amylase levels were also measured (**B**). Bar indicates 5 µm. **C**. The pancreatic mRNAs of WT and IRF2<sup>-/-</sup> mice were prepared by the method of acid guanidium thiocyanate-phenol-chloroform extraction after treated with RNALater (Ambion) for overnight at -80°C, and the expressions of CCK-AR, and CCK-BR were analyzed by Northern blotting with the radio-labeled specific probes. The β-actin expression was shown as control.

**Supplemental Fig. S2** **A**. The schematic structures of mouse trypsinogen genes in the T cell receptor β-chain (TRB) locus. Twenty trypsinogen genes (T1~T20) are found in mouse, but only 12 of them are thought to be expressed, as indicated by filled arrows. The mouse Trb v, d, j genes are shown as open arrows. **B**. The evolutionary pedigree of three human trypsinogens and 12 mouse trypsinogens. Human PRSS1, 2, 3 and mouse Prss1, 2, and 3, and trypsinogen5 are boxed. The pedigree was made using the UPGMA (Unweighted Pair-Group Method with Arithmetic mean) method. The associated number calculated by this method indicates the evolutionary distance, such

that smaller values are more homologous and evolutionarily closer to each other, whereas larger values are less homologous and evolutionarily more distant.

**Supplemental Fig. S3** **A.** The trypsinogen5 mRNA expression levels in indicated tissues were normalized to  $\beta$ -actin expression, and are shown on a log scale. It was expressed at low but accurately measurable levels in the wild-type pancreas and skin, compared to the spleen, liver, and lung. The trypsinogen5 mRNA expressions in pancreas and spleen were up-regulated about 1,000-fold in the IRF2<sup>-/-</sup> mice compared to the wild-type. However, the up-regulations were not affected by further abolishing the IFNAR1. **B.** The promoter activity of trypsinogen5 was examined by placing the 1.1 kb trypsinogen5 promoter region before the Firefly luciferase gene, as reporter in 293T cells. The expression vectors for IRF1, 2, 3, 5, and 7 were co-transfected with the reporter, in the presence or absence of MyD88. The luciferase activity was determined with the dual luciferase assay system. IRF1, 5, and 7 enhanced significantly (\*p<0.02) the trypsinogen5 promoter in the presence of MyD88. **C.** The promoter activities of deletion mutants of trypsinogen5 promoter were measured in the absence or presence of both Myd88, and IRF1 or IRF7 in 293T cells. **D.** The dose-dependent effects of IRF2 expression on the IRF1- and IRF7-dependent trypsinogen5 promoter activations in the presence of MyD88. \*p<0.02 vs. the absence of IRF2.

**Supplemental Fig. S4** The amino acid sequences of major human trypsinogens (PRSS1, 2, and 3), and mouse Prss1, 2, and 3, and trypsinogen5 are aligned. The signal peptidase, enteropeptidase, and

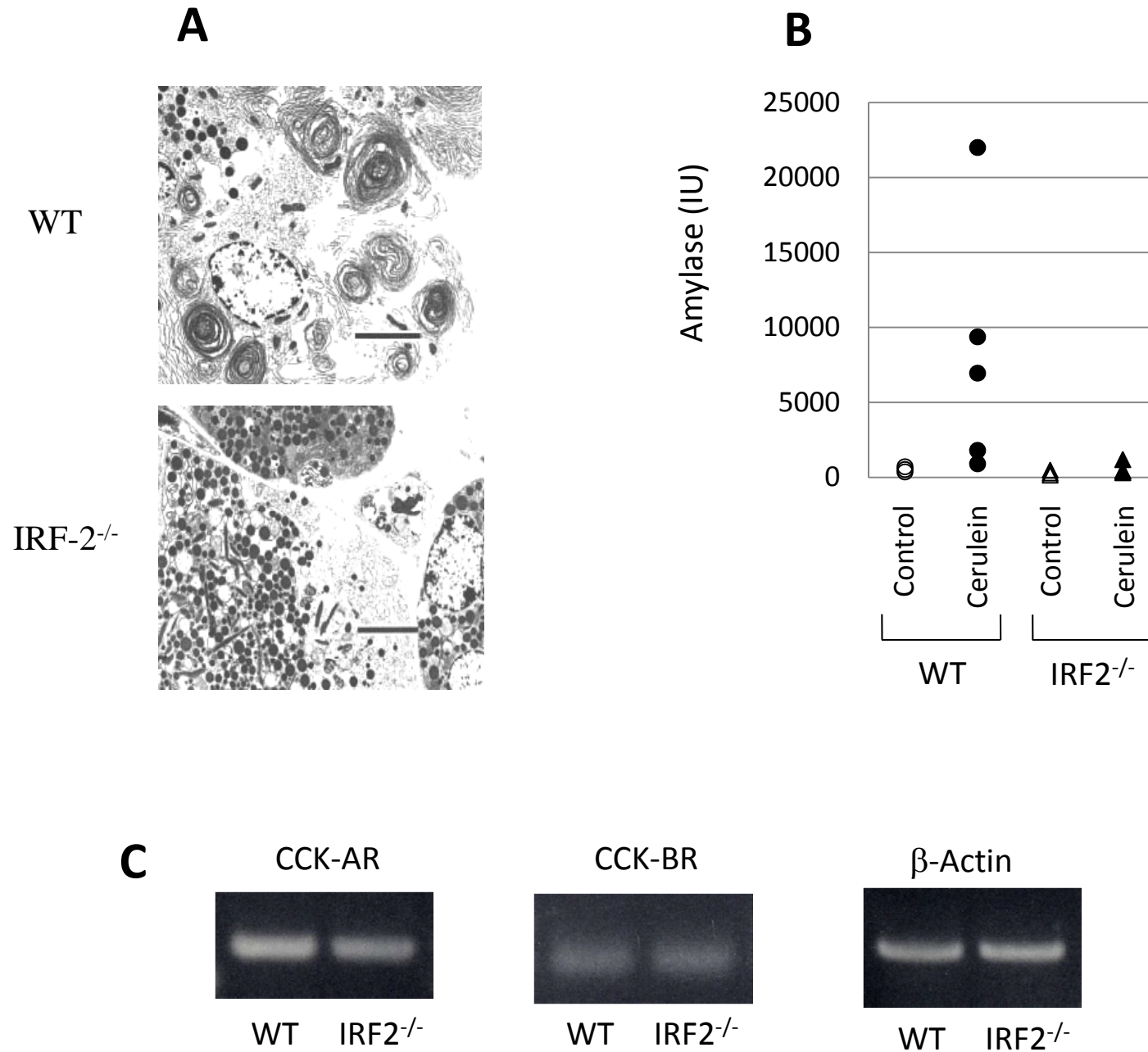
chymotrypsin C cleavage sites are indicated with arrows, and the trypsin autolytic cleavage site is indicated with an arrow head. Active trypsin is generated from trypsinogen, by cleavage at the signal peptide in the endoplasmic reticulum, and at activation peptide in the duodenum. Since mouse trypsinogen5 contains the **triad** (H-D-S) of amino acids essential for the trypsin activity (each amino acid indicated with \*), a signal peptide and an activation peptide in the N-terminal region, this trypsinogen5 is predicted to have enzymatic activity. The inhibitor binding site D<sup>198</sup> is unique in the trypsinogen5, and may confer resistance to trypsin inhibitors, similar to human PRSS3, R<sup>198</sup>. The conserved amino acids are boxed.

**Supplemental Fig. S5** Trypsin activity was monitored by the amount of released p-nitroaniline (pNA) from a specific substrate, measuring spectrophotometric units at 405 nm ( $A_{405}$ ) (Trypsin activity assay kit of BioVision). The activities were dependent on the addition of enteropeptidase (EP), and increased in proportion to the amounts of lysates added to the reaction. Addition of 1, and 2  $\mu\text{g/ml}$  soy bean trypsin inhibitor (SBTI), had no effect on the mouse trypsinogen5 activities observed (**A**). In contrast, the mouse Prss1 activities were inhibited with (SBTI), in a dose-dependent fashion (**B**). **C**. Activation of trypsinogen5 with cathepsin B. The same amounts of 293FT cell lysates transfected with mouse trypsinogen5 (Tryp5) or vector only (Vector) were pretreated with 0.008 units of cathepsin B (CB) in 50 mM acetic acid buffer (pH5.0) for 2h at 37°C, and then subjected to trypsin assay using N-(p-Tosyl)-GPK-pNA as substrate in 100 mM Tris buffer (pH8.0) at 30°C for indicated periods. The amount of pNA released from the specific substrate was measured as trypsin

activity.

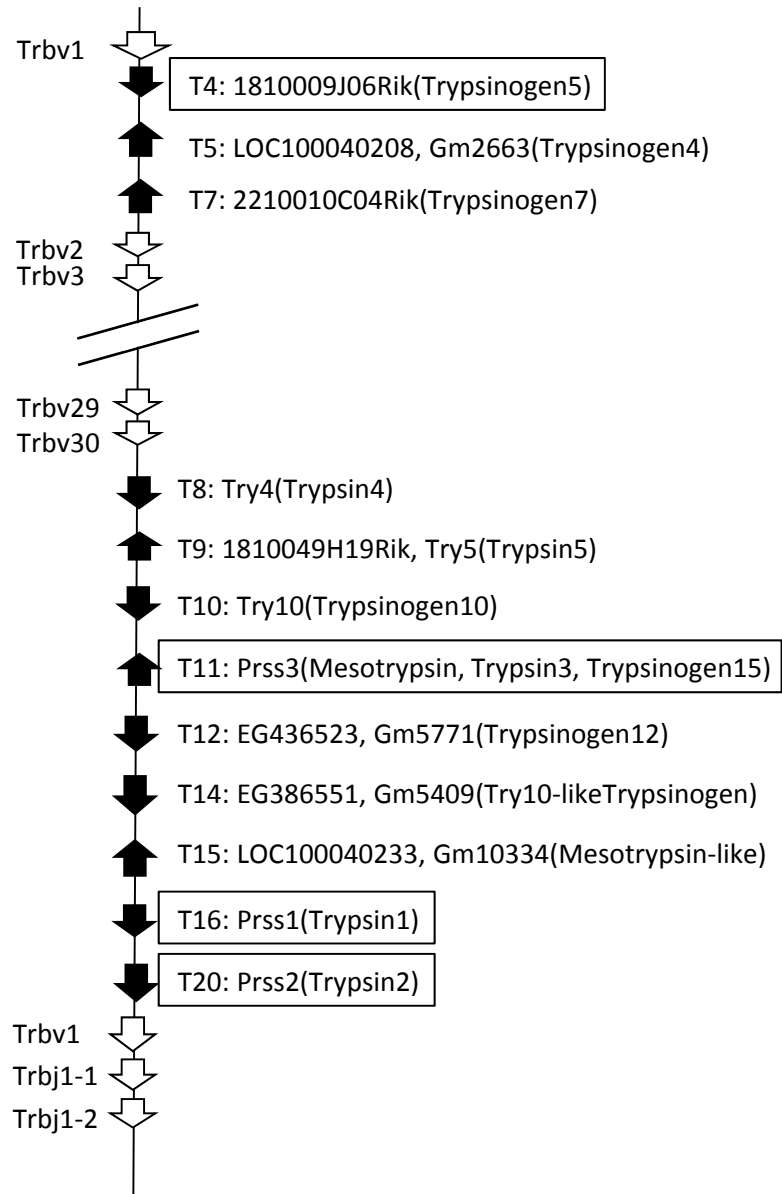
**Supplemental Fig. S6** Pathways for synthetic double-strand RNA (dsRNA), poly(I:C)-dependent signal transductions in WT (A) and in IRF2<sup>-/-</sup> (B) mice. The IRF2<sup>-/-</sup> pancreatic acinar cells susceptible to pancreatitis are loaded with a large number of zymogen granules, including Trypsinogen5, expressed by transcriptional activation by IRF5 and IRF7. pIC induces type I IFN production (I-IFN) and the I-IFN activates transcriptions of ISGs including MDA5, RIG-I, and TLR3. The increased MDA5, RIG-I, and TLR3, induce cell death via IPS-1, and TRIF. The leaked Trypsinogen5 from dying acinar cells, is activated to Trypsin5 by released proteases such as cathepsinB, or nearby enteropeptidase. Cell death is exacerbated since the Trypsin5 is resistant to the major pancreatic trypsinogen inhibitor, Spink3. The cell death amplification (enhancing loop) leads to severe pancreatitis. →: stimulatory signals, ↗: Transcriptional activations.

Supplemental Fig.S1

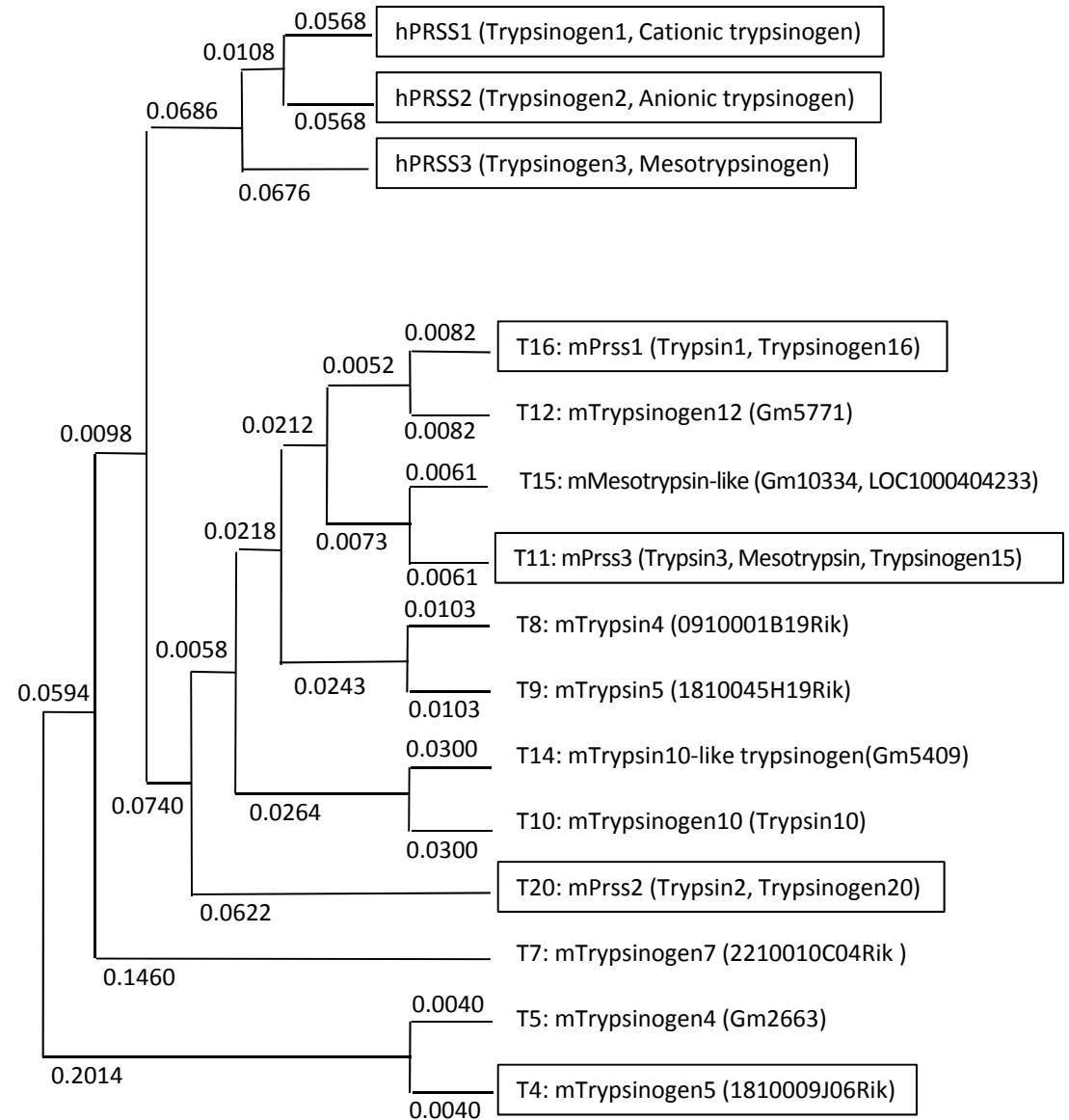


# Supplemental Fig.S2

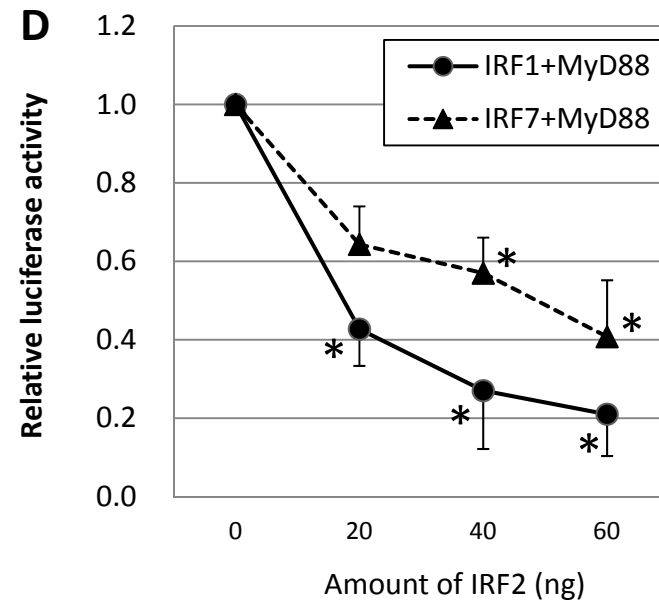
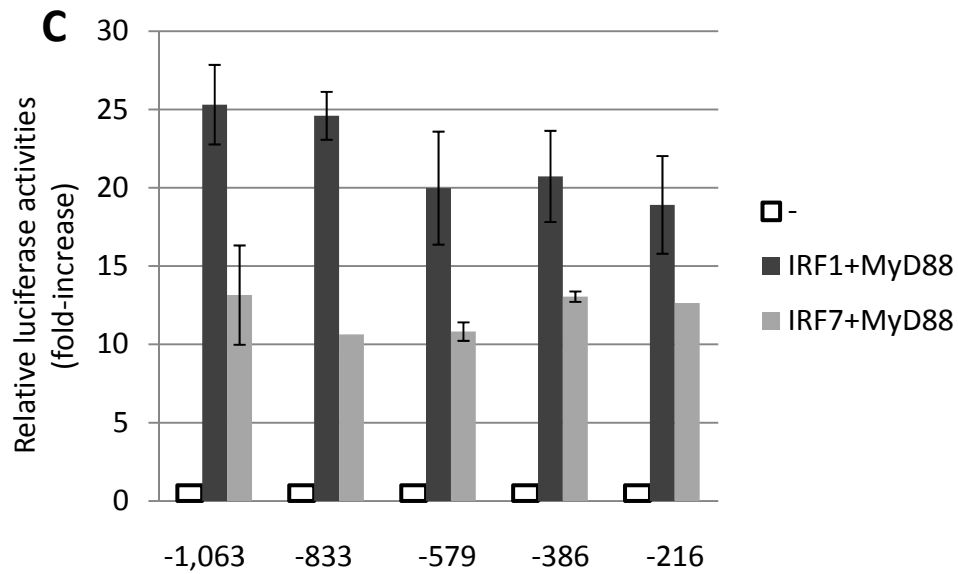
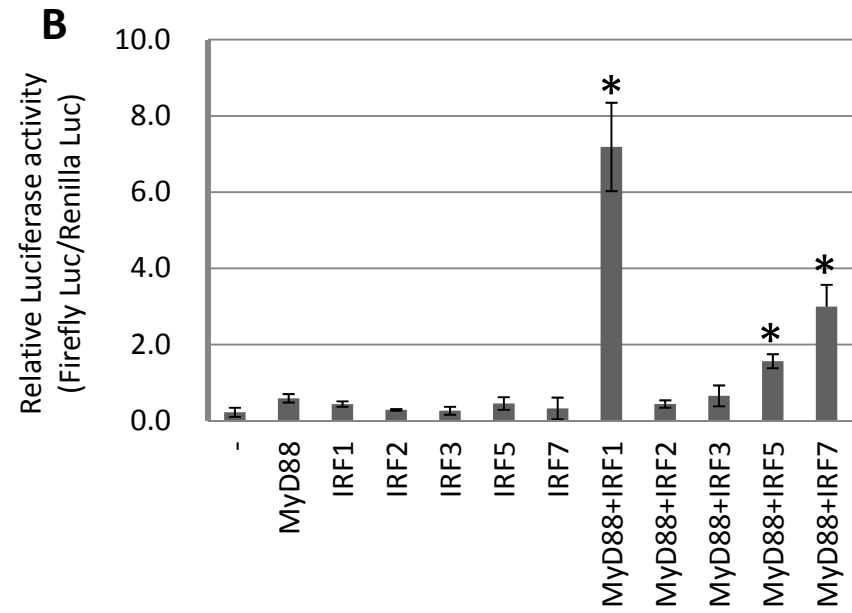
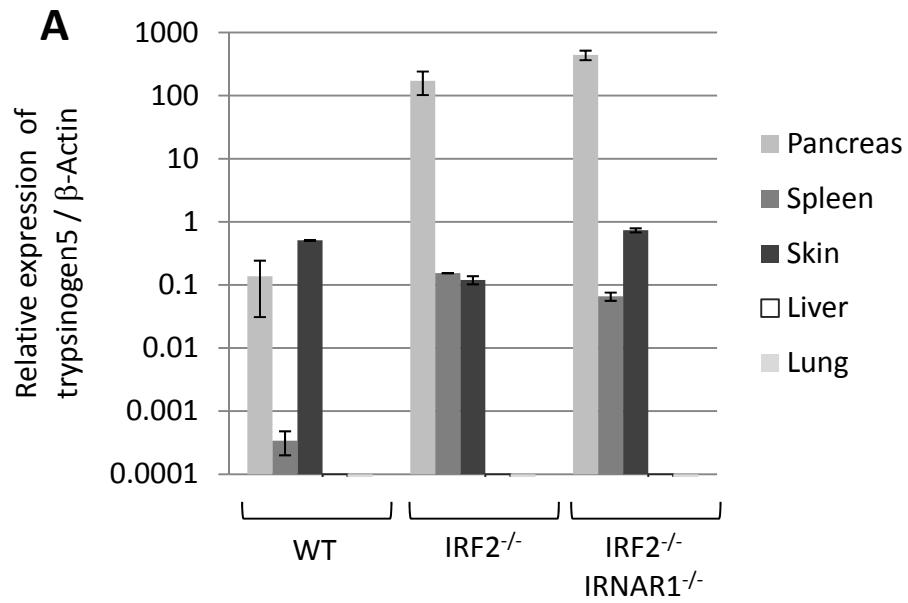
## A. Mouse Chromosome 6



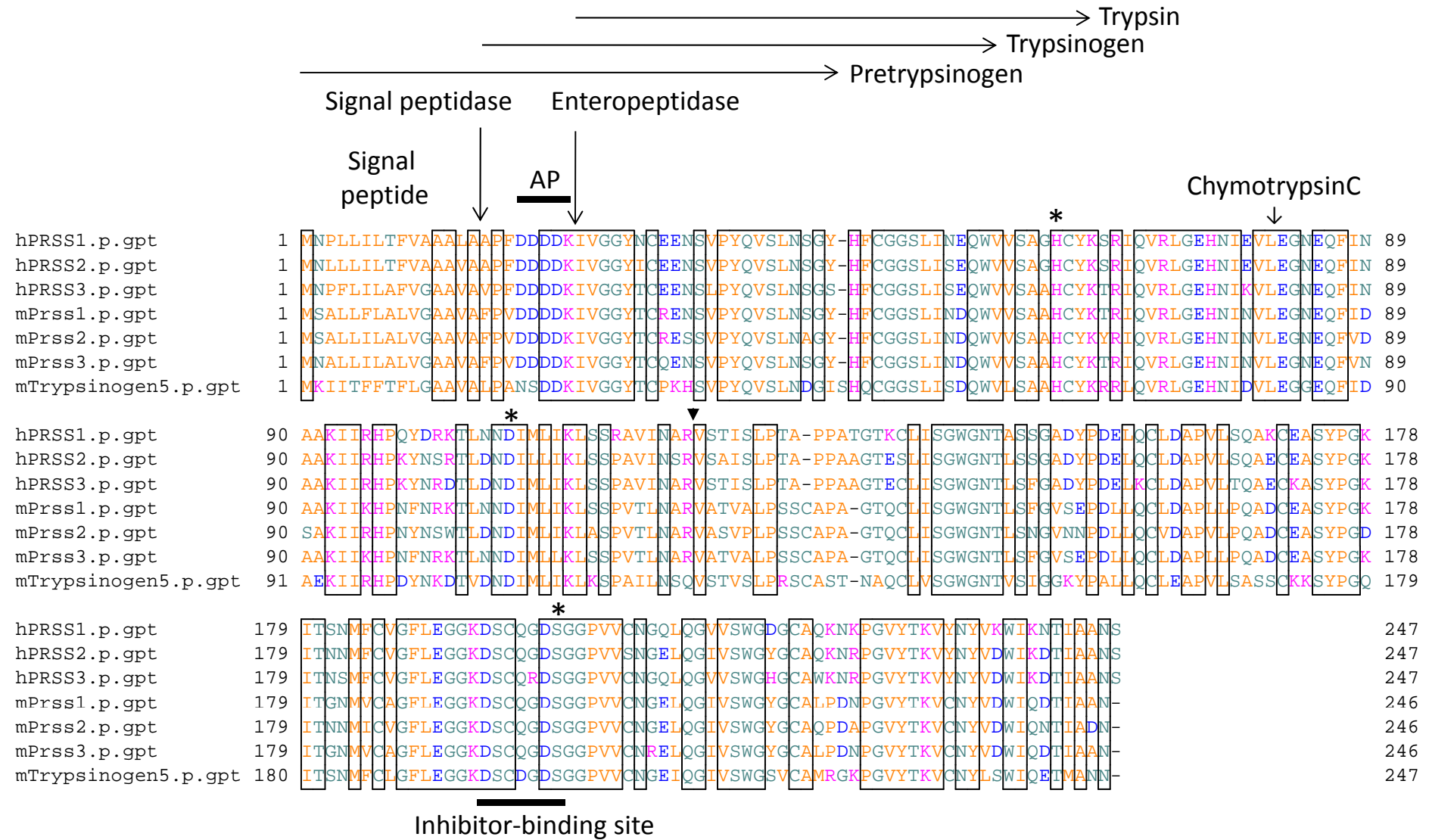
## B. Evolutional Pedigree of Trypsinogens



# Supplemental Fig.S3



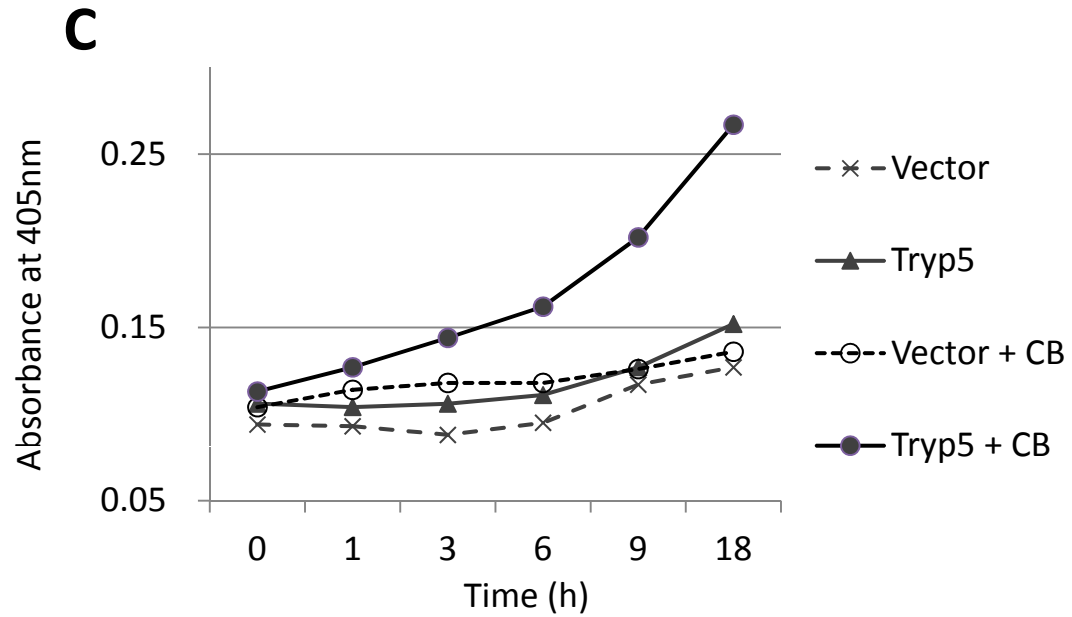
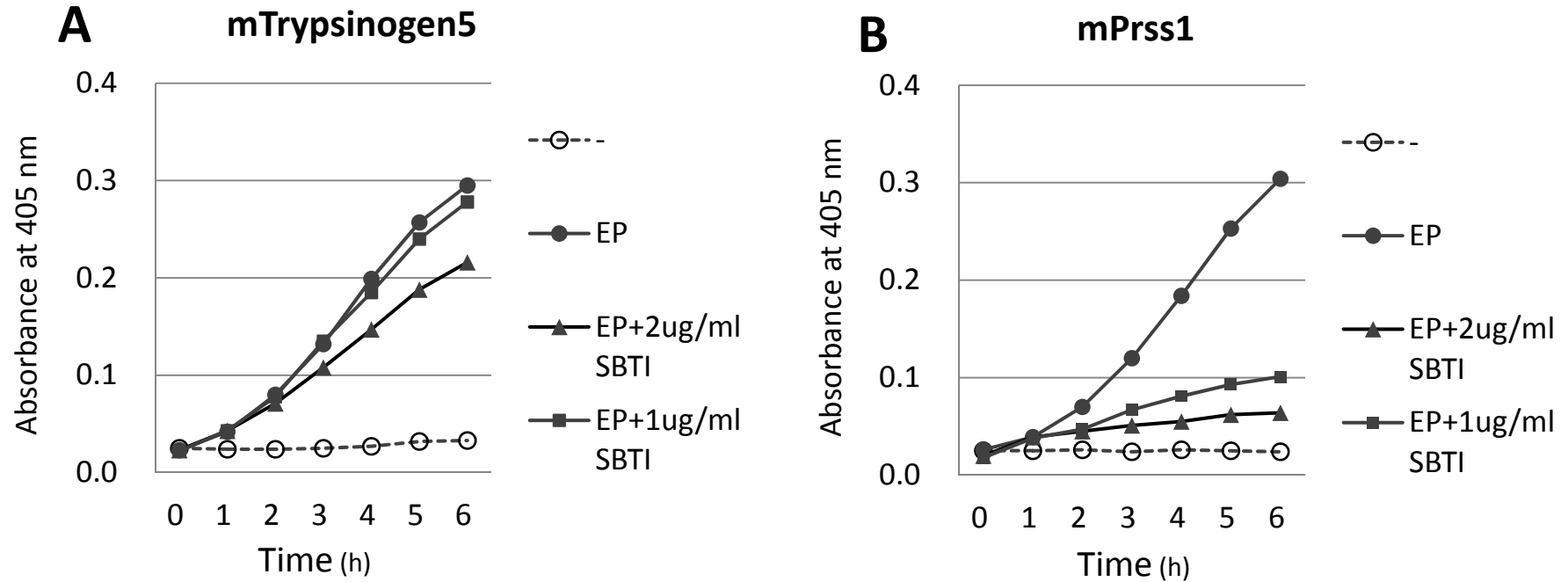
# Supplemental Fig.S4



AP: Activation peptide

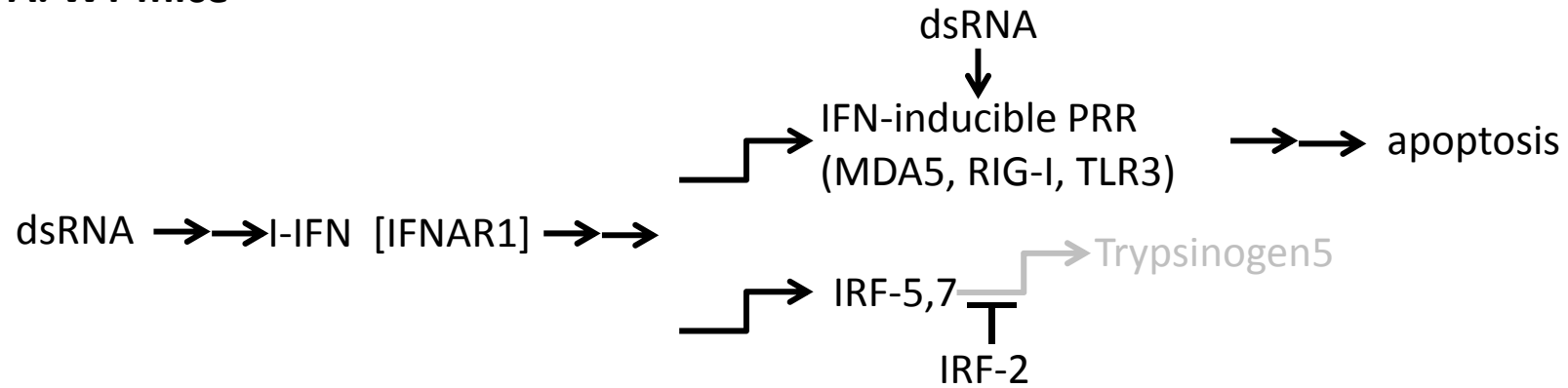
\* : Triad (H-D-S)

Supplemental Fig.S5

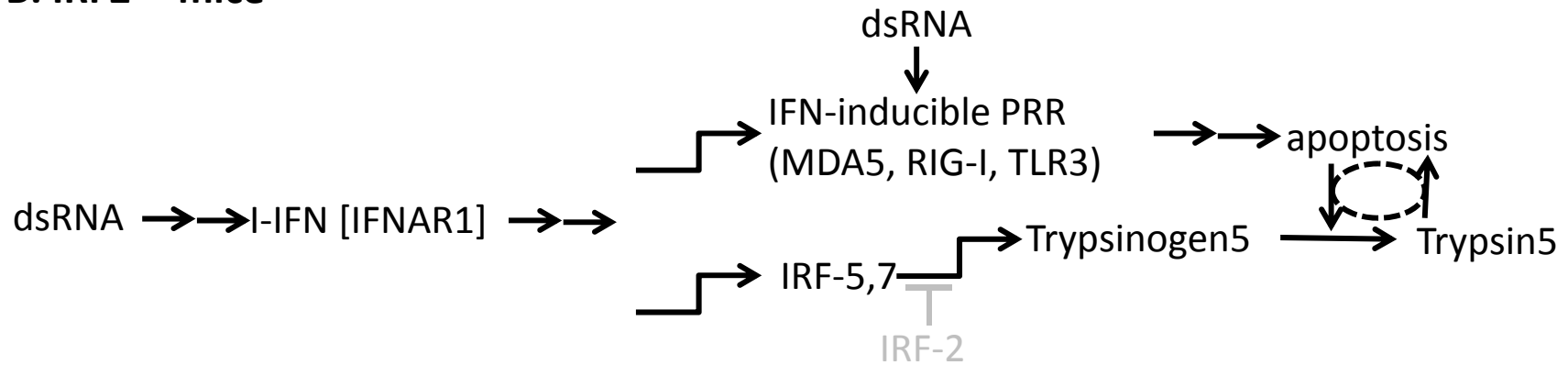


Supplemental Fig.S6

**A. WT mice**



**B. IRF2<sup>-/-</sup> mice**



**Supplemental Table S1.** Significantly up- and down-regulated genes in IRF2<sup>-/-</sup>  
(Affymetrix unit)

<b>Genes</b>	<b>WT (-)</b>	<b>WT (poly I:C)</b>	<b>IRF2<sup>-/-</sup> (-)</b>	<b>IRF2<sup>-/-</sup> (poly I:C)</b>
<b>Trypsinogen 5 (1810009J06Rik)</b>	<b>80</b>	<b>69</b>	<b>14345</b>	<b>15470</b>
Fetuin β (Fetub)	14	15	926	1623
3-Hydroxy-3-methylglutaryl-Coenzyme A synthase 2 (Hmgcs2, HMG-CoA synthase)	23	240	1375	777
<b>Annexin A10 (Anxa10)</b>	<b>11</b>	<b>11</b>	<b>647</b>	<b>427</b>
Ep1 (epithelial progenitor 1)	10	12	303	111
Lectin, galactose binding, soluble 9 (Lgals9)	90	625	1369	1629
<b>α-2-HS-glycoprotein (Ahsg, Fetuin-A)</b>	<b>10</b>	<b>12</b>	<b>157</b>	<b>591</b>
Transmembrane 4 superfamily member 4 (Tm4sf4)	58	64	783	349
Guanylate binding protein 2 (Gbp2)	22	1064	258	1230
regenerating islet-derived 3γ (Reg3g)	268	4511	2756	2758
Macrophage activation 2 like (Gbp6, guanylate binding protein 6)	17	177	174	349
Lipocalin 2 (Lcn2)	28	146	283	217
Group specific component (Gc, Vitamin D-binding protein)	30	21	186	577
<b>S100 calcium binding protein G (S100-G)</b>	<b>58</b>	<b>19</b>	<b>114</b>	<b>252</b>
Immunoglobulin kappa chain variable 8 (Igk-V8)	25	455	24	7
Carbonic anhydrase 3 (Car3)	152	1301	103	49
Complement factor D (adipsin)	157	707	56	38
Immunoglobulin joining chain (Igj)	30	168	25	11
<b>Galanin (Gal)</b>	<b>879</b>	<b>1057</b>	<b>213</b>	<b>71</b>
Cxcl13 (chemokine (C-X-C motif) ligand 13)	82	806	29	60
Immunoglobulin lambda variable 1 (Iklv1)	18	147	25	14
Solute carrier family 38, member 5 (Slc38a5)	1533	1683	143	196

Upper fourteen annotated genes were up-regulated more than 10-fold in IRF2<sup>-/-</sup> mouse. The up-regulation of trypsinogen 5 more than one hundred-fold by inactivating IRF2 gene was noteworthy, because trypsinogens are reported to play important roles to develop pancreatitis. The three Ca<sup>2+</sup>-binding proteins are also highlighted. Lower eight genes were down-regulated more than 10-fold in IRF2<sup>-/-</sup> mouse. Galanin is reported to mediate the Cerulein-induced pancreatitis (1).

**Supplemental Table S2.** Expressions of IFN-signaling molecules  
(Affymetrix unit)

<b>Genes</b>	<b>WT (-)</b>	<b>WT (poly I:C)</b>	<b>IRF2<sup>-/-</sup> (-)</b>	<b>IRF2<sup>-/-</sup> (poly I:C)</b>
<b>IRF1</b>	<b>35</b>	<b>286</b> ↑	<b>44</b>	<b>361</b> ↑
IRF3	97	113	136	114
IRF4	19	16	10	15
IRF5	34	47	36	46
IRF6	114	148	197	171
<b>IRF7</b>	<b>26</b>	<b>375</b> ↑	<b>107</b>	<b>224</b> ↑
IRF8	32	81	43	54
IRF9	44	191	88	237
IPS-1	109	113	121	123
TRIF	53	55	51	53
<b>MyD88</b>	<b>31</b>	<b>311</b> ↑	<b>77</b>	<b>297</b> ↑
TIRAP	23	46	36	47
<b>MDA5</b>	<b>35</b>	<b>921</b> ↑	<b>76</b>	<b>733</b> ↑
<b>RIG-I</b>	<b>47</b>	<b>538</b> ↑	<b>93</b>	<b>458</b> ↑
TLR1	9	9	10	6
TLR2	55	151	55	133
<b>TLR3</b>	<b>13</b>	<b>98</b> ↑	<b>24</b>	<b>118</b> ↑
TLR4	20	26	26	27
TLR6	15	18	14	12
TLR7	6	21	16	12
TLR8	8	9	10	9
TLR9	42	80	40	36

The DNA microarray analysis indicated that IRF1, IRF7, MyD88, MDA5, RIG-I, and TLR3 were significantly up-regulated with the poly(I:C) in the pancreas of IRF2<sup>-/-</sup> mice.

**Supplemental Table S3.** Relationship among relevant gene expressions, cell death, and pancreatitis

	WT		IRF2 <sup>-/-</sup>		IRF2 <sup>-/-</sup> /IFNAR1 <sup>-/-</sup>		IRF2 <sup>-/-</sup> /TRIF <sup>-/-</sup>	
	-	Poly (I:C)	-	Poly (I:C)	-	Poly (I:C)	-	Poly (I:C)
Granule retention	-	-	+++	+++	+++	+++	+++	+++
Trypsinogn5	-	-	+++	+++	+++	+++	+++	+++
TLR3/TRIF	+	+++	+	+++	+	+	-	-
MDA5/RIG-I/IPS-1	+	+++	+	+++	+	+	+	+++
Cell death	-	+	-	+	-	-	-	+
Enhanced cell death	-	-	-	+++	-	-	-	+
Pancreatitis	-	-	-	+++	-	-	-	+
Serum amylase	-	-	-	+++	-	-	-	+

IRF2<sup>-/-</sup> caused abnormal granule retention (+++), and conspicuous expression of Trypsinogen5 (+++), and the characteristics were not rescued by further destroying IFNAR1 or TRIF. There were at least two cell death pathways; the TLR3/TRIF and the MDA5/RIG-I/IPS-1, and the high expressions of TLR3/TRIF or MDA5/RIG-I/IPS-1 (+++) caused cell death. In addition, high expressions of spink3-resistant trypsinogen5 (+++) are required for the enhanced the enhanced cell death led to pancreatitis with elevated serum amylase (+++).